UCRL-10499

University of California

Ernest O. Lawrence Radiation Laboratory

ULTRACENTRIFUGE
PHOTOELECTRIC SCANNER, SPLIT-BEAM

Berkeley, California

DISCLAIMER

Research and Development

UCRL-10499
UC-37 Instruments
TID-4500 (19th Ed.)

UNIVERSITY OF CALIFORNIA
Lawrence Radiation Laboratory
Berkeley, California

Contract No. W-7405-eng-48

ULTRACENTRIFUGE PHOTOELECTRIC SCANNER, SPLIT-BEAM

Kenneth W. Lamers

October 9, 1962

ULTRACENTRIFUGE PHOTOELECTRIC SCANNER, SPLIT-BEAM

Contents

ULTRACENTRIFUGE PHOTOELECTRIC SCANNER, SPLIT-BEAM

Kenneth W. Lamers

Lawrence Radiation Laboratory
University of California
Berkeley, California

October 9, 1962

ABSTRACT

This report describes an electromechanical scanner for displaying optical density changes when a light-absorbing material such as virus, protein, or nucleic acid is sedimenting in the centrifugal field of an ultracentrifuge; that is, a high-speed centrifuge employing an optical system. These materials absorb some of the light transmitted by the optical system, thereby projecting an image that varies in intensity with distance from the center of rotation. This image, which consists of alternate light pulses from a reference and a sample cell, is scanned by a photomultiplier. Subsequent circuitry separates the reference and sample pulses and takes their logarithmic difference. The system, therefore, compensates for non-uniform illumination and other optical imperfections. The logarithmic difference is displayed on a chart recorder, the paper moving in synchronism with the scanner. Optical density (concentration) is thereby displayed as a function of radius. An additional trace simultaneously records the derivative of the density profile. Other modes record the image of each cell before optical correction. An internal calibration feature permits absolute measurement of optical density.

ULTRACENTRIFUGE PHOTOELECTRIC SCANNER, SPLIT-BEAM*

Kenneth W. Lamers

Lawrence Radiation Laboratory
University of California
Berkeley, California

October 9, 1962

I. INTRODUCTION

An ultracentrifuge is a high-speed centrifuge employing an optical system.[1] In this application it is used for displaying optical density changes when light-absorbing material such as virus, protein, or nucleic acid is sedimenting in a centrifugal field.

This paper describes a photoelectric scanning system developed for ultracentrifuge studies. It is an improved version of a scanner developed earlier.[2] The principal modification is that a differential readout has been incorporated to compensate for such optical imperfections as non-uniform illumination or dirty lenses. The new system also differs in the sense that the electronics is responsive to light intensity, as opposed to the light-time integral of the previous scheme.

The optical imperfections referred to above can be minimized in some cases, but the process is tedious and time-consuming. Furthermore, the correction is not permanent because the lenses become coated with oil deposits from the centrifuge drive. Therefore, it seems more practical to compensate electronically for the optical distortions, and make corrections for the conditions prevailing at the time of scan.

---

*This work was done under the auspices of the U. S. Atomic Energy Commission.

II. GENERAL CONSIDERATIONS

One way of compensating for optical distortion is to add a reference cell to the ultracentrifuge rotor. This provides a means for comparing the sample path with another related to optics only. The difference between them can be used to "iron out" the variations due to optical imperfections, yielding a profile that is truly representative of sample concentration.

It should be pointed out that this technique is subject to error if the transmittance profiles of the reference and sample cells (including solvent) are different. It is necessary, therefore, that the profiles be matched, and that they be equally influenced by extraneous deposits. The cells must be cleaned prior to each run so that they will not be susceptible to accumulated deposits. Since both cells are enclosed by a common window material, matching is not a practical problem. In general, the differential method is much more convenient than cleaning and adjusting less accessible components.

Assuming a reference cell, the next concern is that of shape, size, and location. Both cells, obviously, must be located at the same radius relative to the center of rotation, but their angular separation is somewhat arbitrary. Small angular separations minimize environmental differences, but they also reduce the time separation between alternate light pulses. This is especially important at high speeds, where more severe requirements are placed upon the electronic circuitry required to identify and separate pulses. Elaborating, a 1.8-deg cell separation corresponds to a time separation of only 5 μsec when rotating at 60 000 rpm.

Small angular separations have another disadvantage; namely, the photomultiplier slit must be short enough to prevent its "seeing" both cells at the same time. Reduced slit lengths result in less illumination, and so the signal-to-noise ratio is less favorable.

The present setup uses 2-deg cells with an angular separation of 2.5 deg, a value compatible with the electronic problems of pulse separation. At some wavelengths, however, the light intensity is inadequate for satisfactory signal-to-noise ratio, and so more illumination is desirable. One solution is to increase three dimensions, namely; slit length, cell angles, and cell separation. The alternative is to find light sources of higher intensity at the wavelength of interest.

As for cell shape, this has less significance with a split-beam system, provided that the slit length is shorter than any part of the cell images.

III. DESIGN PHILOSOPHY

A number of approaches to split-operation were apparent, but the most attractive was to modify the original single-beam system. This would have permitted retention of proven circuitry, allowing concentration on those features peculiar to split-beam. Subsequent considerations, however, indicated than an alternate approach is more practical, and so the original scheme was abandoned for reasons that follow.

Referring to Fig. 1, a block diagram of the earlier single-beam system, the basic design is seen to be quite simple. A low-pass filter extracts the pulse envelope, yielding an output proportional to the light-time product. The filter, a sharp-cutoff, maximally flat type, gives good resolution while at the same time providing high attenuation to the undesired spectra resulting from the sampling process.[3] The principal disadvantage is that the filter output is proportional to the duty cycle, the fractional time that the input pulses are present. Assuming a 4-deg cell, the usual value for single-beam, the filter output level is roughly 1% of the peak input pulse height. This results in low output levels; thus, drift and pickup problems become more severe. The light-time response is also limiting, and imposes requirements upon the cell window shape.

In split-beam operation, the cell angles are normally 2 deg. This lowers the duty cycle to half the single-beam value, reducing the filter output proportionately. This, in turn, aggravates filter stability requirements, active types being necessary to obtain the rolloff necessary at the slower scanning rates.

The foregoing considerations indicated the desirability of a system responsive to pulse height and independent of duty cycle. The one finally decided upon uses holding circuits.[4] The circuitry evolved employs switching circuits that alternately charge each of two holding capacitors. These are charged to the peak pulse amplitude through a diode. The discharge time constant is comparatively long, producing an average output level much higher than that of the low-pass filter type. This increased level is very effective in minimizing drift.

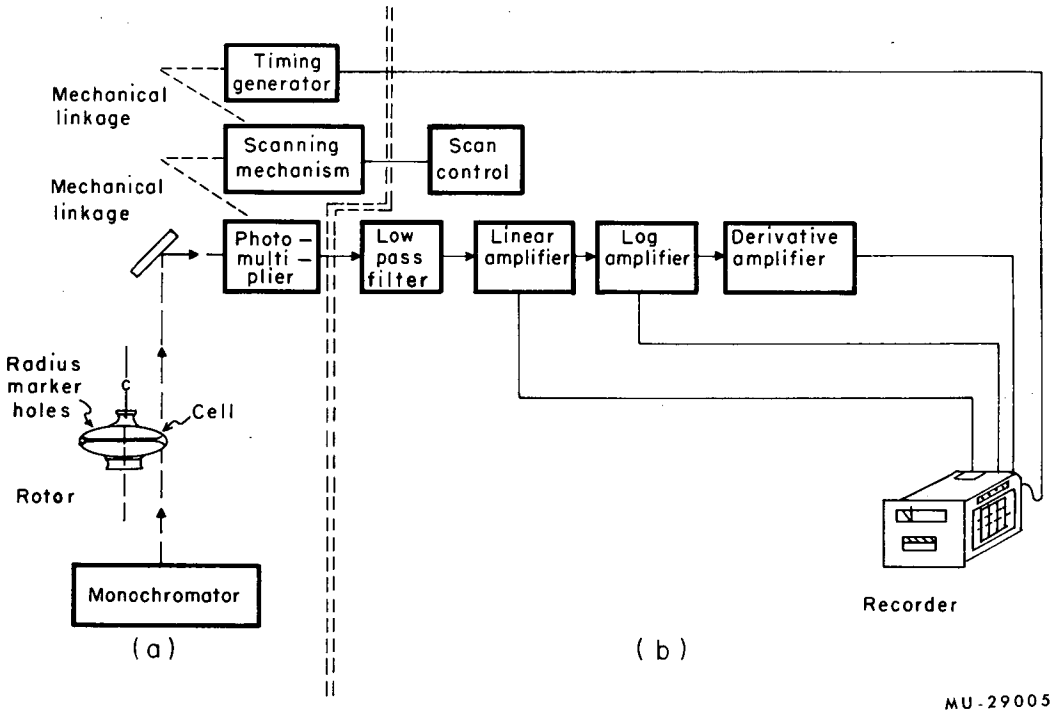

Fig. 1. Block diagram of the single-beam system, showing important electrical and mechanical components of the photoelectric scanner: (a) ultracentrifuge, and (b) control console.

IV. SYSTEM DESCRIPTION

Figure 2 is a simplified block diagram of the system evolved. When compared to the single-beam system in Fig. 1, it will be noted that the scanning and recording mechanisms are essentially the same; therefore, discussion is restricted to those features unique to the split-beam system developed. Referring again to Fig. 2, a photomultiplier with defining slit[5] scans the image at a constant speed.[6] It accepts light samples as the centrifuge makes them available, generating pulse amplitudes proportional to the light intensity producing the pulse. The pulse duration is related to centrifuge speed, cell angle, and slit length.

The nature of the pulses generated by the photomultiplier is shown in Fig. 3. These actual photographs of oscilloscope traces show the duration, amplitude, and separation of the pulses with the scanner stopped at various positions along the image (see Fig. 4).

Figure 3(a) shows the pulse-pairs generated when the scanner is stopped at a position of the image that corresponds to solvent in the reference cell and an optical density of 1 within the sample cell. The reference cell offers no appreciable attenuation, and so the pulse amplitude generated is 10 times that of the sample cell.

In brief, the photomultiplier generates a pulse when the centrifuge rotor makes light available. When scanning the cell images, the photomultiplier "sees" two quick light bursts, the first due to the reference cell, the second to the sample.[7] This is followed by a quiescent period that is much longer than the interval between pulses.

It should be pointed out, however, that the entire image does not consist of pulse-pairs. For example, the rotor includes two radius-marker holes, as shown in Fig. 4. These are displaced 180 deg from the centerline between cells, and are used to determine the magnification factor. While the scanner is "observing" the image of either radius marker, the rotor allows only one light burst per revolution, as shown by Fig. 3(d).

Assuming that the photomultiplier generates a train of pulses, the next problem is to decipher which cell (or radius marker) is responsible for a given light impulse. The sample and reference pulses do not occur simultaneously, and so they cannot be compared at their time of occurrence. One of the pulses must be stored for comparison with its corresponding "mate."

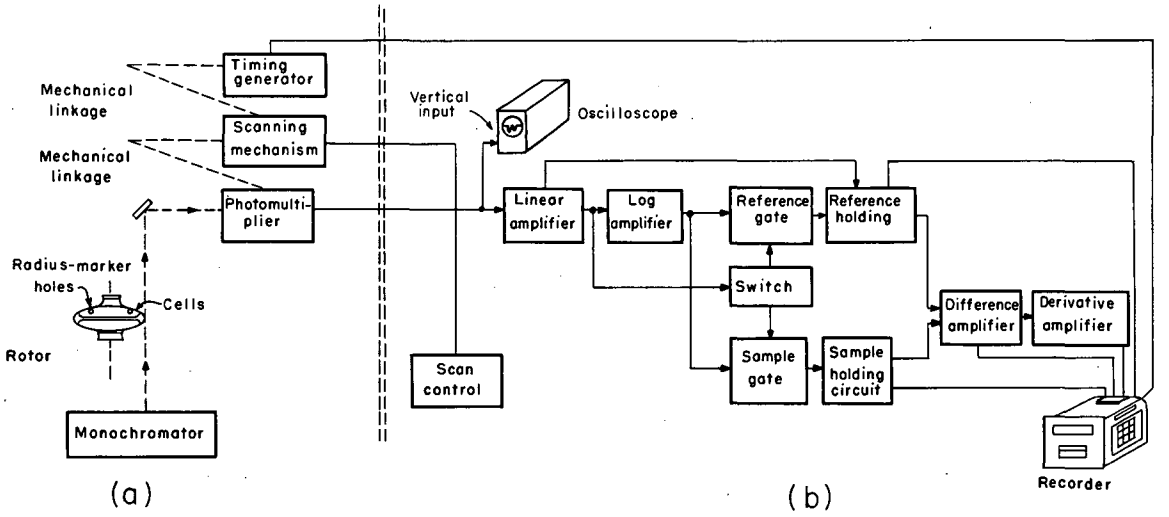

Fig. 2. Block diagram of the split-beam scanning system: (a) ultracentrifuge, and (b) control console.

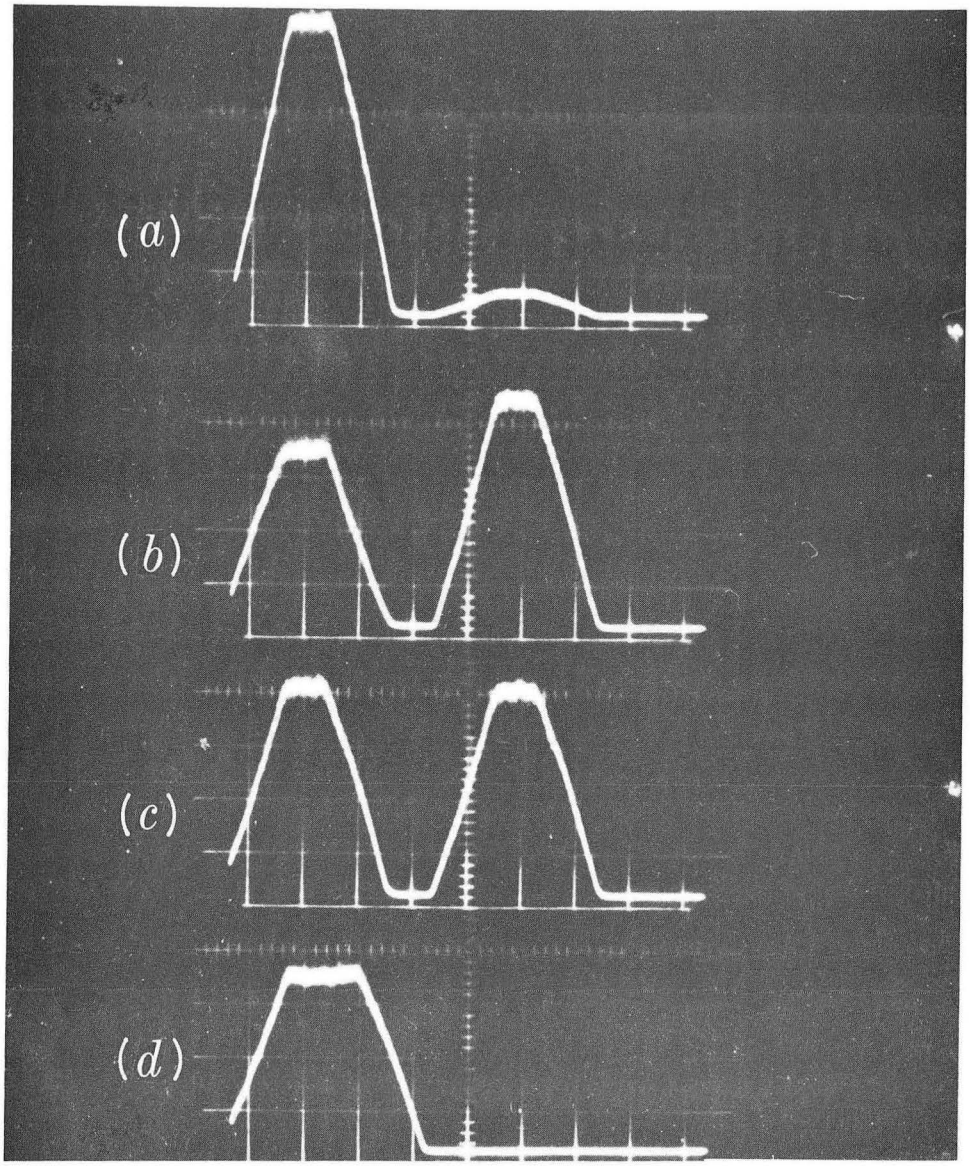

ZN-3599

Fig. 3. Oscilloscope traces, showing photomultiplier pulses (inverted) with the scanner stopped at various positions (refer to Fig. 4):
(a) Scanner positioned at a radius yielding two light bursts per revolution. The first pulse is due to the reference cell solvent, water; the second to the sample cell. (b) Scanner positioned at a radius corresponding to the air-solvent boundary within the reference cell. The reference pulse is slightly attenuated by the meniscus. Sample pulse is not attenuated appreciably because light passes through the air space. (c) Scanner positioned at a radius corresponding to the air space of both cells. The window material is common to both cells, so each pulse is the same height. (d) Scanner positioned at a radius corresponding to radius-marker hole R1 (see Fig. 4). Pulse width is slightly longer, and related to the diameter of R1. Photomultiplier "sees" only one light burst per revolution.

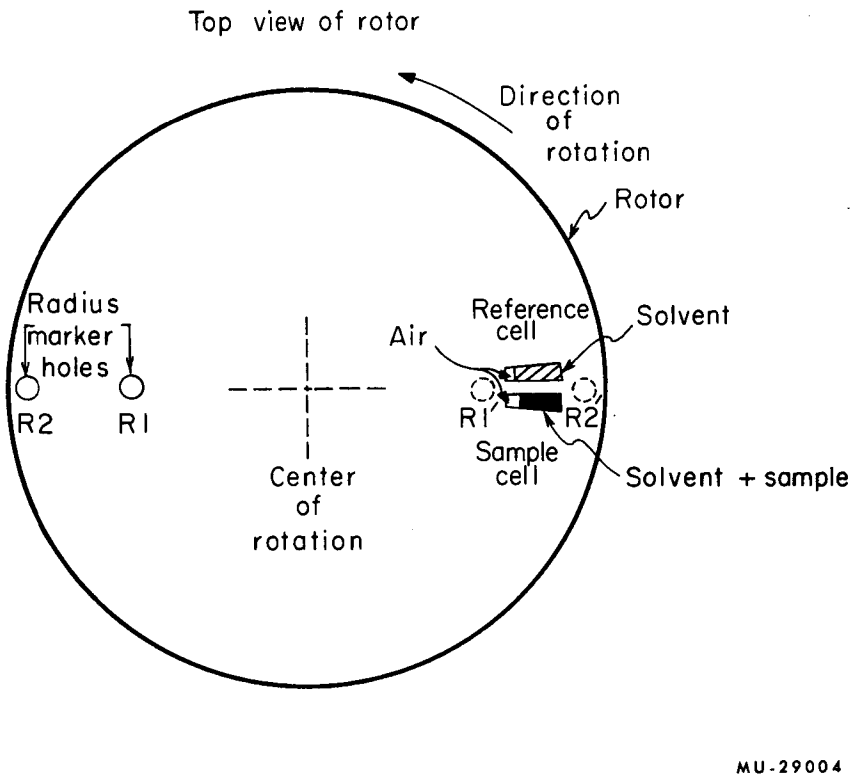

Fig. 4. Top view of rotor, showing the radius-marker holes, and the reference and sample cells. The holes are displaced a half revolution from the centerline between cells. R1' and R2' are nonexistent. They are included to indicate that the radius-marker images straddle the cell images when the rotor is turned a half-revolution. The cells are not filled completely, and so an air space forms at the inner radius.

The storage feature makes it necessary to route each light pulse to the proper place, and this in turn requires some method for sensing which cell (or radius marker) was responsible for that pulse.

There are a number of ways to correlate light impulse with rotor position. The most obvious methods use extraneous sensing elements to detect rotor position and effect switching at the proper time. These, however, require additional sensing elements; they also create alignment problems. In view of practical considerations, all such systems were rejected in favor of one that performs logic on the basis of information received at the photomultiplier only. This is feasible because cell separation is not 180 deg, permitting identification to be deduced from pulse time-separation.

Referring to the functional block diagram of Fig. 5, the linear amplifier output pulses activate a gating chain consisting of two squaring amplifiers, a one-shot, and a switch.[8] The net result is that the switch opens either one of the two gates, but never both simultaneously.

If we assume that the gates are in one of two states, the question arises as to when the transition is made from one state to the other. This is best explained by reference to Fig. 6, which shows the various pulse and gating relationships throughout the system. The circuitry is designed so that reference gate R is normally open to the first pulse coming through. The trailing edge of that pulse activates the switch, closing the reference gate for 400 μsec. This transition simultaneously opens the sample gate (previously closed) for 400 μsec, permitting the following pulse to pass through the sample gate. At normal operating speeds, this time interval is comparatively short and permits only one pulse to pass through the sample gate. Furthermore, the time interval is short enough to ensure that the subsequent pulse gets through the sample channel if, and only if, it happens to be the "mate" of the original pulse.

Suppose, for the moment, that the first pulse coming through is associated with the sample cell. The reference gate is open, and so the first pulse inadvertently gets through the reference gate. This is rectified 400 μsec later, however, because the one-shot returns to its original state, which allows the next pulse to pass through the reference gate. Since that pulse is produced by the reference cell, gating is restored to normal.

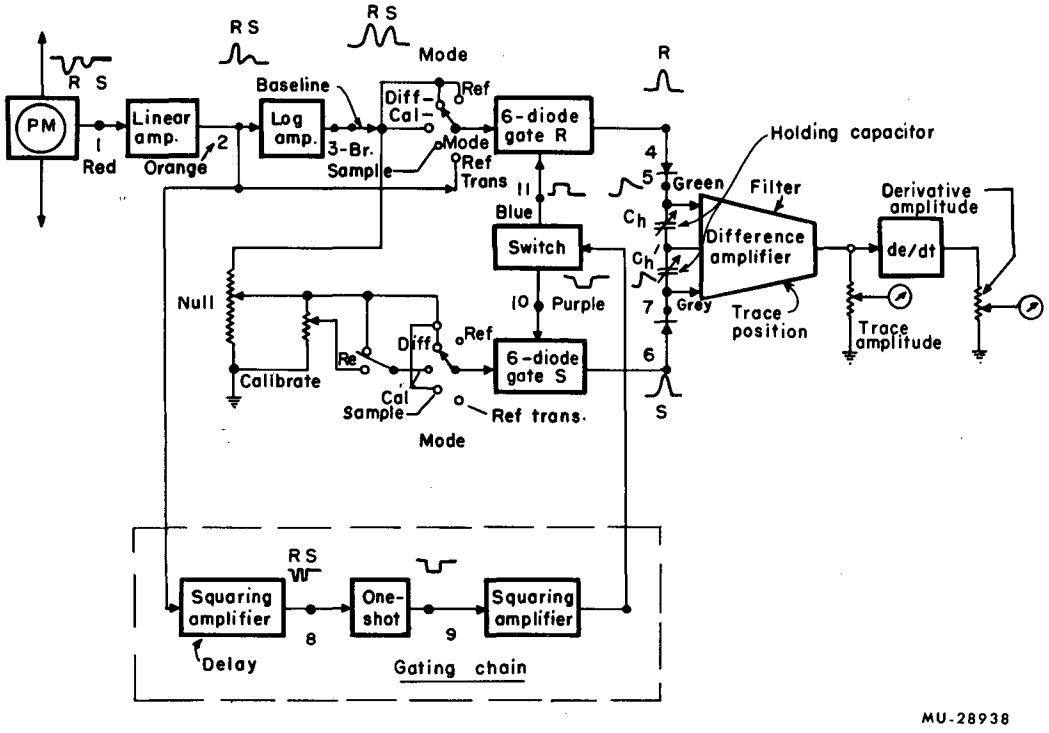

Fig. 5. A functional block diagram illustrating the manner in which a pulse-pair is separated with the Mode switch in Difference position. Monitor jacks are provided at test points indicated in color. Re (center of diagram) identifies the relay contacts that vibrate in Cal position. Filter (upper right) determines high-frequency response. Trace position (right) determines input bias. The magnitude of capacitors C_h and C_h' (right) is selected to suit the rotor speed being used. Delay (low center) controls the average clipping level.

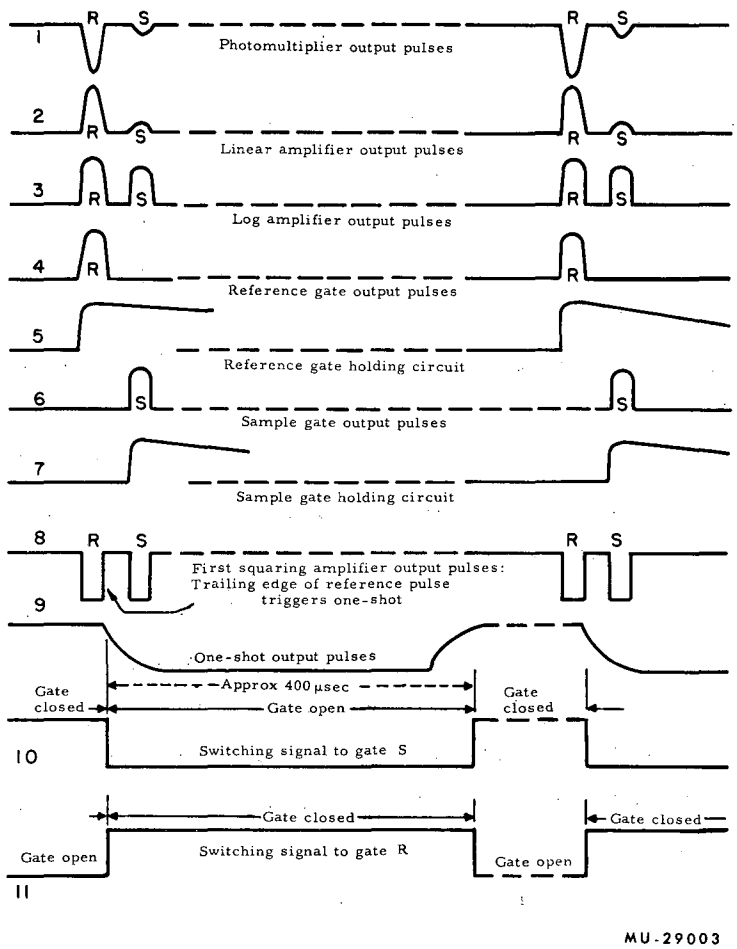

Fig. 6. Time relationships of the various pulses throughout the system, Mode switch in Difference position. The numbers correspond to the test points indicated in Fig. 5.

Consider next those scanner positions in which the photomultiplier "sees" a radius marker only. In that event, it generates only one pulse per revolution, and this is automatically routed through the reference gate. This is because the first pulse always goes through the reference gate, as described above. Since the subsequent pulse is 360 deg later, and is always later than 1 msec, no pulse appears during the 400 μsec period during which the sample gate is open.

With regard to gate types, the 6-diode gate was selected because it has low leakage when the gate is closed. This is especially important at high optical densities where a small percentage of leakage introduces a large error. This type also has other virtues; e. g., the switching component does not appear in the output, the gain is close to unity, and the linearity is excellent.[9] The bilateral properties do require a series diode for peak charging, but this is not a serious limitation.

Referring again to Fig. 5, when the Mode switch is in the Difference position the pulses are separated so that the reference pulses pass through Gate R and the sample pulses through Gate S. The output from each gate charges its holding capacitor C_h through a series diode. The latter is a unilateral device which permits the associated holding capacitor to charge up to the peak pulse amplitude, retaining that value with a slowly decaying time constant until the next pulse comes along. This holding capacitor maintains the average output voltage at a high level, thereby minimizing the effects of drift, pickup, and noise. The discharge time constant, adapted to centrifuge speed, is determined by the holding capacitor size and the effective shunt resistance.

Figure 5 shows that the holding capacitor size is a function of centrifuge speed. A number of factors must be considered to determine the correct value, but these may be reduced to two discrete effects: (a) The charging time constant must be short enough to ensure that the capacitor charges to the peak pulse amplitude, and (b) the discharge time constant must be long enough to maintain the average output voltage at a suitable level without impairing the high-frequency performance. In view of these considerations, a selector switch (Holding Capacitor), is included to permit one to select the optimum time constant for each speed.

The voltages appearing across each holding capacitor are applied to a difference amplifier. The amplifier output, proportional to the difference between reference and sample-hold voltages, is applied to the Visicorder.[10] An intervening attenuator (Trace Amplitude) controls the deflection magnitude.

The difference amplifier output is also applied to an operational amplifier with an appropriate time constant for taking the derivative. The derivative output is applied to another Visicorder channel, and so both outputs, the function and its derivative, are recorded in time coincidence.

A number of photographs are included here. Figure 7, for example, is an overall view of the ultracentrifuge (as supplied by the manufacturer).[11] Figure 8 illustrates the scanning mechanism when viewed from above the centrifuge. Figure 9 shows the scanning mechanism intact, but removed from the centrifuge. Figure 10 shows the scanning mechanism disassembled. Figure 11 is a front view of the Control Console, at present adapted to include the operating controls for two centrifuges. The upper panel contains the circuitry relevant to a single-beam scanner. The inherent simplicity is useful, but it will probably be replaced by the split-beam type, the panel of which is shown in Fig. 12.

The appendix includes split-beam schematics and a number of derivations which verify that the system is linearly responsive to the optical density of the sample. This is true despite channel gain differences, non-uniform illumination, and a limited region of logarithmic response.

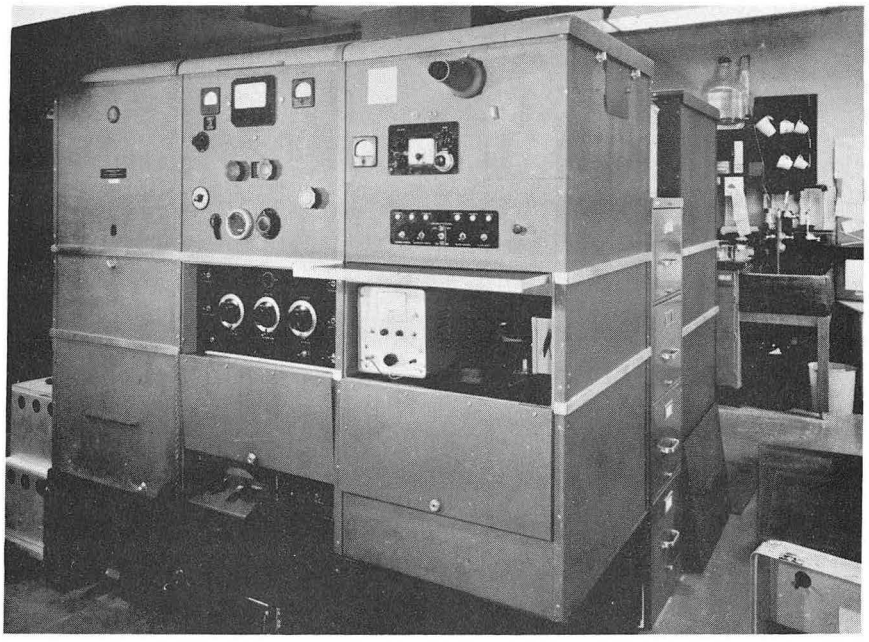

ZN-3502

Fig. 7. An overall view of the ultracentrifuge as supplied by the manufacturer.

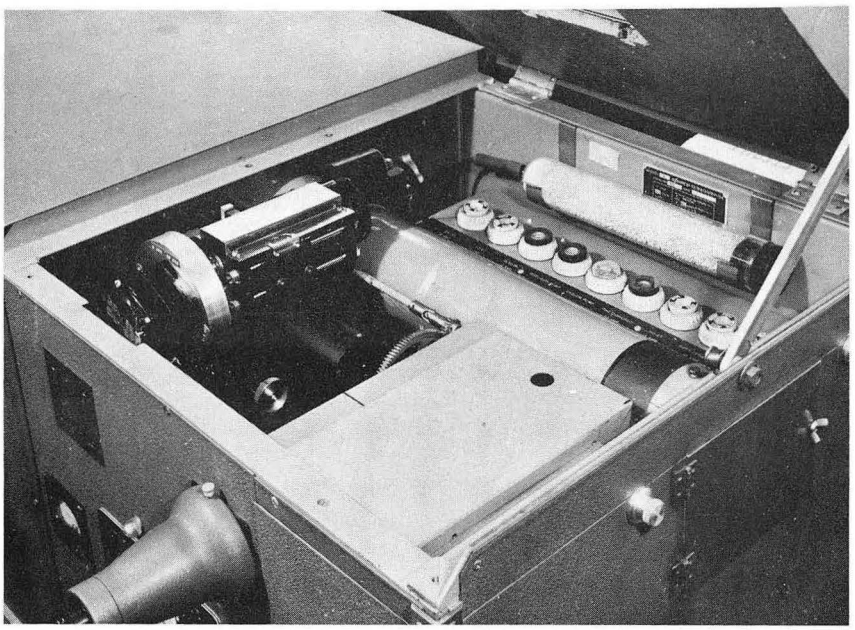

ZN-3503

Fig. 8. A photograph of the drive unit mounted in the ultracentrifuge. This view is from the right-hand end of the instrument and from slightly above the top. The lid of the ultracentrifuge, opened for this picture, clears the scanning mechanism and is normally closed to prevent room light from interfering with its operation.

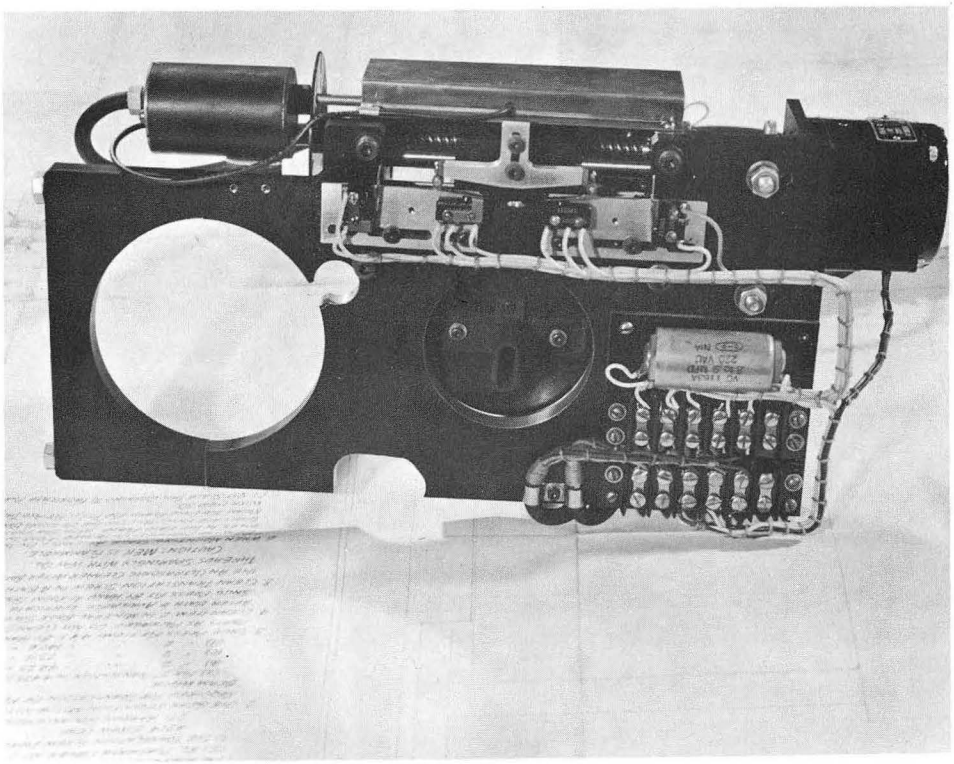

ZN-3570

Fig. 9. A view of the scanning mechanism removed from the ultracentrifuge (prior to adding the slit selector and the variable speed transmission). Light rays passing through the optical system (perpendicular to the plane of the photograph) enter through the vertical slot, which acts as a light shield, and then through a narrow vertical slit to the photomultiplier.

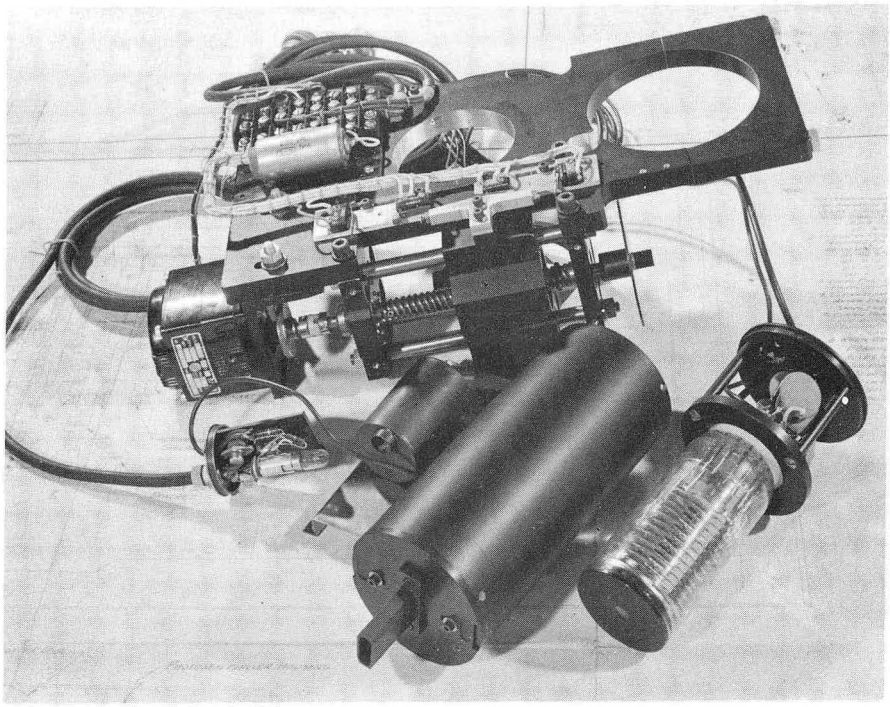

ZN-3499

Fig. 10. The scanning unit, partially disassembled to show some of the basic components: the photomultiplier and its housing; the light for the timing generator; the lead screw, coupling, and motor; and the cam and safety switches mounted on the support bracket (the slit selector and the variable speed transmission are not shown).

ZN-3501

Fig. 11. A front view of the Control Console, at present adapted to include the operating controls for two ultracentrifuges. The upper panel contains circuitry for a single-beam unit, early version. Directly below is the split-beam operational unit, then the Visicorder. Below the Visicorder, a scan control panel includes separate controls for each mechanism. The bottom panel is a power supply for both photomultipliers. Directly above it is an adapter panel for operating each photomultiplier at a different voltage.

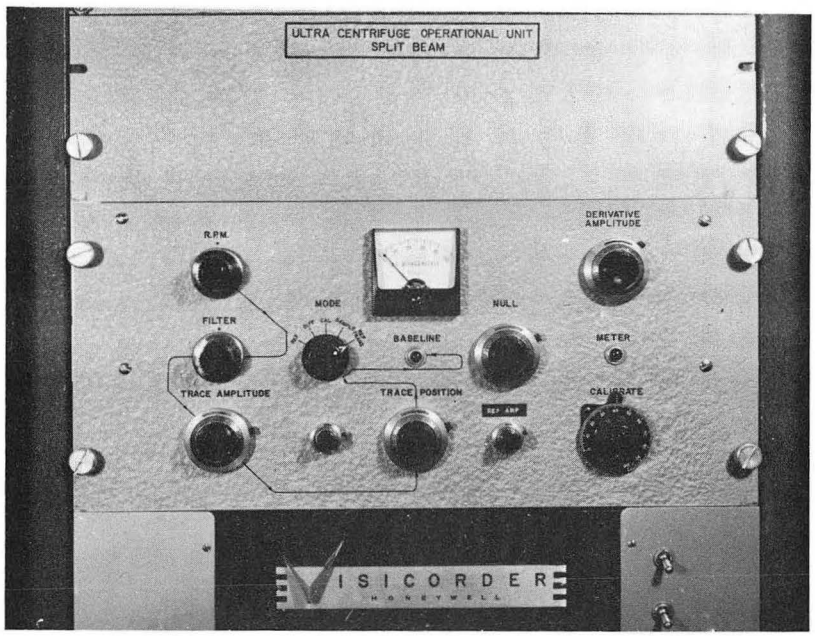

ZN-3500

Fig. 12. Split-beam operational unit. The controls are arranged functionally with the operating sequence indicated by a flow-type diagram. The RPM designation has been changed to "Holding Capacitor." The small duo-dial below the Mode switch is the Delay control.

V. OPERATION

Some of the more obvious controls have been covered in the discussion above; the remainder are best explained in conjunction with the operating procedure.

The usual procedure is to adjust the photomultiplier voltage for 2-V output pulses, with the scanner positioned at the air space. This ensures that the photomultiplier is operating in a linear region, that the switching circuits are triggered with an adequate signal, and that the logarithmic voltage compressor operates about the desired input level. The Holding Capacitor control is then set for the corresponding centrifuge speed, the Mode switch placed in Reference position, and a scan is recorded. The resulting trace represents the reference-cell density profile when devoid of optical correction. It also includes the radius markers for reasons described above.

The reference profile is examined, and the Trace Amplitude, Trace Position, and Filter controls modified accordingly. The Filter control determines the high-frequency response of the difference amplifier, and thereby influences resolution and output noise. If used judiciously in combination with slower scanning speeds, a high degree of resolution may be obtained even with comparatively noisy photomultiplier pulses.

The Mode switch is now changed to Difference position, the scanner is positioned at the air space (indicated by equal pulse heights on the oscilloscope), and Null is adjusted until depressing Baseline does not influence the recorded level. This Null adjustment balances the gates under common optical density conditions, indicating the position of zero density difference.

The instrument is now ready for operation, subsequent tracings recording the difference in optical density between cells. The true zero baseline can be verified by depressing the Baseline button at various scanner positions. The position to which the spot returns when crossing the air space is the true baseline, and it will differ somewhat from the apparent baseline when the scanner is in Start Position. This feature has been added because the baseline shifts when a region is being scanned in which light intensity is inadequate to maintain synchronization. It is possible to minimize this shift, even nullify it, but there is no assurance that the adjustment is permanent. To promote accuracy, it seems more desirable to refer to a baseline which we know exists during the time that synchronization pulses are present. Depressing Baseline does not disrupt synchronization; it merely disconnects the input pulses from both gates.

The foregoing procedure has prepared the instrument to record Difference traces, but cross-checks are available to provide assurance that the system is operating properly. For example, the Mode switch should be changed to Sample and the scanner operated. The resulting trace represents the sample-cell density profile, uncorrected for optics, and it should not have radius markers. If it does, the trouble may be due to an incorrect Delay setting. If the gating circuits switch too soon, the sample-hold circuit charges up to that residual level of the radius-marker pulse which exists at the time of switching. This can be corrected by advancing the Delay control, adjusting for minimum radius-marker height with stable traces when the Mode switch is in Sample position.

Anomalies sometimes appear in the reference-cell traces, as shown in Fig. 13. If so, the trouble may be due to light scattering. Light scattered by the cells, or by a radius marker, sometimes produces spurious pulses when the scanner is positioned in the vicinity of either radius marker. These pulses are displaced one-half revolution from the desired pulses, and are usually apparent on the oscilloscope. When exaggerated by the logarithmic amplifier, they have appreciable magnitude, as shown in Fig. 14 (center pulse, upper trace), charging the reference holding circuit to a considerable voltage. This effect can be detected if the oscilloscope is connected to monitor the reference holding circuit. If scattered light is responsible, spurious peaks will appear as shown in Fig. 15(a) lower trace. This effect is apparent only if the holding-circuit discharge time constant is short enough so that its decayed voltage at the 180-deg pulse is less than the logarithmic amplitude of the spurious pulse arriving at that time.

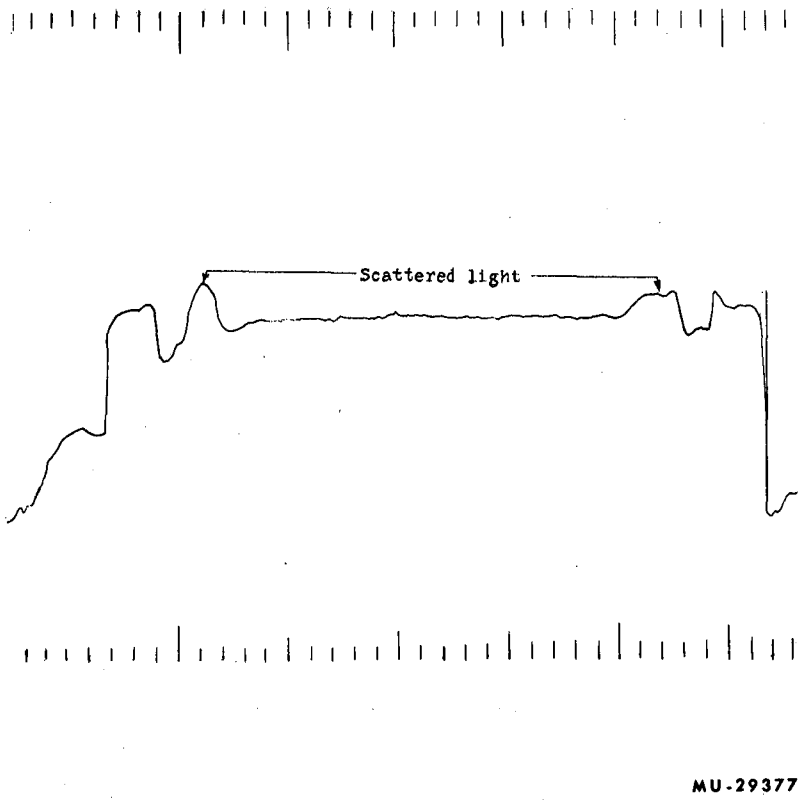

Fig. 13. Tracing shows the reference-cell profile distortion resulting from scattered light. The holding-circuit discharge time constant is too short, as shown in Fig. 15(a).

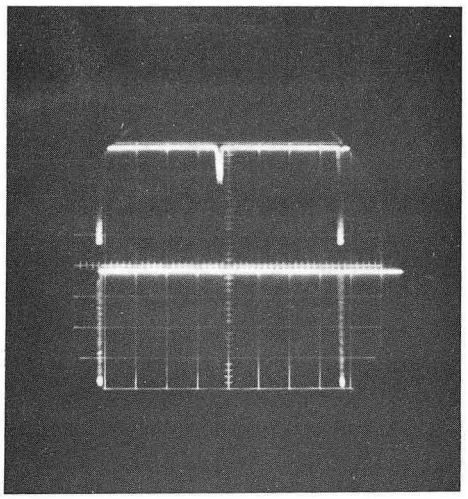

ZN-3606

Fig. 14. Single exposure of an oscilloscope trace, dual-beam, taken with the scanner positioned at one of the radius-marker holes. Scattered light is prevalent, producing spurious pulses when the two cells appear 180 deg later than the radius marker. The upper trace is the log output (inverted), exaggerating the almost invisible pips that appear in the center of the lower trace (the photomultiplier output pulses). The amplitude of the pulses from the scattered light is approximately 1% of that from the radius-marker pulses.

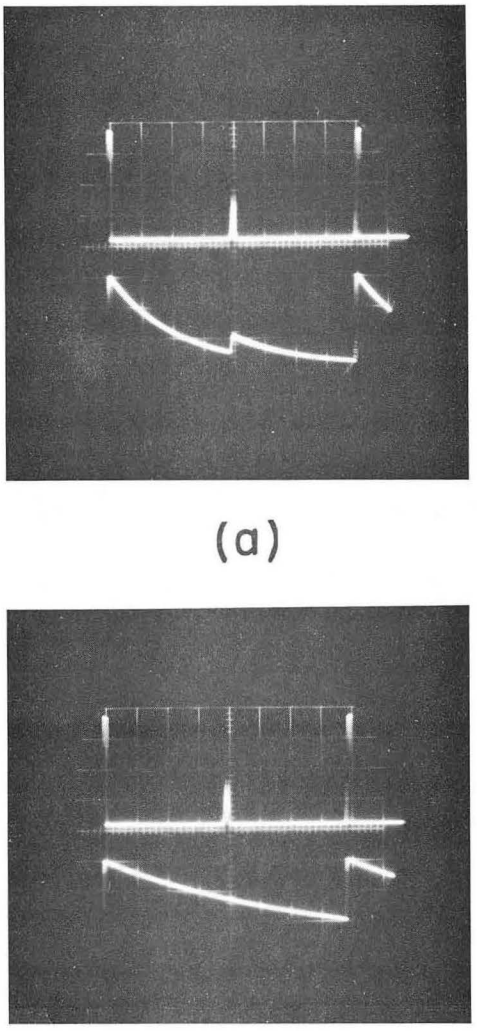

Fig. 15. Oscilloscope traces, dual-beam, showing the reference holding-circuit response to scattered light pulses: (a) The upper trace is the log output; the lower trace is the reference-hold voltage. The holding-circuit discharge time constant is short, and so the spurious pulses increase the average voltage output. (b) Some as (a) except that the holding-circuit time constant has been increased. The holding circuit no longer responds to the spurious pulses.

VI. MODES OF OPERATION

Referring to Fig. 5, it will be noted that the Mode switch has five positions, each connecting both gate inputs to the desired function. When placed in Reference position, all pulses are applied to the reference gate input; none is applied to the sample gate input. The net output, due to the reference gate only, consists of pulses from one of two sources, the reference cell or either radius marker, dependent upon scanner position.

The second, or Difference, position has been described above. Reviewing, all input pulses are applied to both gate inputs, and the appropriate pulses appear at the output of each gate.

The third position (Calibrate) is provided to facilitate density calibration. When used in this mode, the scanner is positioned at the air space to provide pulse-pairs of equal height. The system is then nulled in the Difference position, and the Mode switch shifted to Calibrate. The recorder output will now switch between two discrete positions, one of them corresponding to zero density difference (see Fig. 16). The other spot position depends upon the Calibrate dial setting, empirically calibrated in terms of optical density. In this mode, all pulses are applied to the reference-gate input. They are also applied to the sample-gate input, but a relay causes the latter input to alternate between the input pulses and an attenuated version thereof.

The Calibrate dial performs the electrical equivalent of attenuating the pulse coming through the sample cell. When the spot vibrates between its limits, we see positions corresponding first to the unattenuated value, then to the attenuated pulse. The attenuated pulse amplitude is related to the setting of the Calibrate dial.

The fourth position (Sample) applies all pulses to the sample gate input. The output consists of sample pulses only. Inversion occurs when used in this mode, and so the Visicorder galvanometer is reversed to maintain a consistent presentation.

The fifth position (Reference Transmittance) applies an attenuated version of the linear amplifier output to the reference gate input. The reference gate output consists of pulses from either a radius marker or the reference cell, depending upon scanner position. The linear version of the reference cell facilitates focusing and alignment of the optics. This is because it accentuates those changes that are normally minimized by the logarithmic circuit. The log circuit, on the other hand, is useful in exaggerating changes that occur at small input amplitudes, relative to normal amplitude pulses.

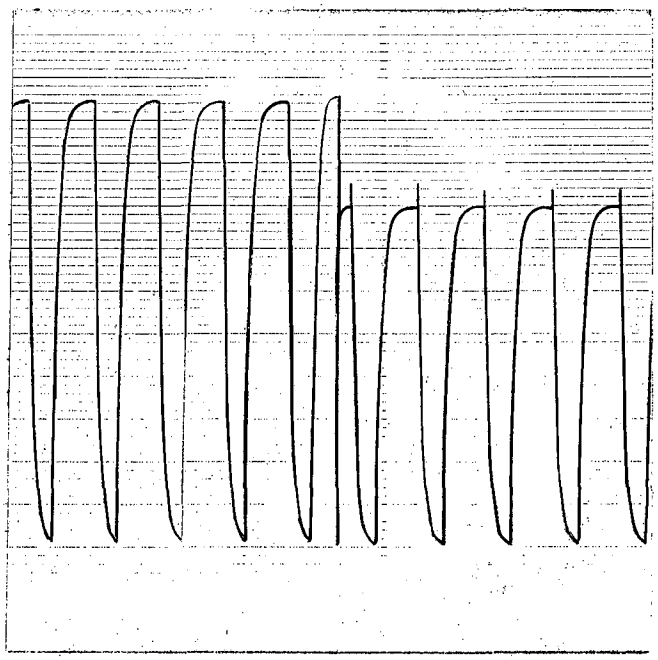

MU-29378

Fig. 16. Tracing with the Mode switch in Calibrate. The scanner is positioned at the air space to give equal pulse amplitudes from each cell. A relay causes the Visicorder spot to switch between two discrete limits, one of them dictated by the Calibrate dial setting. The chart drive produces a recording as shown. The figure indicates the vibration limits resulting from two arbitrary settings of the Calibrate dial.

VII. SINGLE-BEAM OPERATION

The primary purpose of the Delay control is to set the pulse level at which switching occurs, but it is also useful for converting to single-beam operation. To clarify, the Delay control determines the average level about which clipping occurs in a squaring amplifier. If advanced too far, the linear amplifier output pulses do not pass through the necessary excursion levels, and so the following circuits are not activated. This feature has utility if we wish to obviate the switching circuits for use with a single-sector cell. In that case, we merely advance Delay to the maximum clockwise position and place the Mode switch in Reference. Operation is now single-beam. Unlike the previous single-beam system, it responds to peak light intensity only; it does not respond to the light-time integral. If operated with a double-sector cell the recorded profile is a hybrid. The level recorded at a given scanner position represents the higher of the two "mates."

When returning to split-beam operation, it is necessary to readjust the Delay control properly. Since maladjustment can produce errors in the recorded traces, a discussion seems pertinent. For example, if the control is set so that the delay time is too short, switching occurs with the reference-cell pulse level at a high amplitude. The sample gate, opened at that instant, responds to the residual level of the reference pulse, charging the sample-hold capacitor with an erroneous pulse. If the reference residual at the time of switching is less than the "mate," the error is negligible when compared with the average area enclosed by the holding circuit voltage-time representation. The degree of error is related to the angular separation between cells, and is less for smaller separations.

If the Delay control is advanced too far, switching becomes erratic, especially when illumination is non-uniform.

The non-switching type of operation just described offers several advantages. First, the baseline does not shift in the absence of input pulses. Second, the gating circuits are not activated, and so there is no possibility that the switching component will appear in the output. The inherent simplicity of the system is quite attractive in many cases.

It should be pointed out, however, that there are times when single-beam performance can be improved by allowing the switching circuits to activate, just as they do with split-beam. Switching can be used to discriminate

against scattered light pulses. For example, single-beam operation is obtained with the Mode switch in Reference position. None of the pulses is applied to the sample gate in this mode, and so the spurious pulses appear in the output only if they can get through the reference gate. The trick is to make the gating length longer, so that the spurious pulses arrive when the reference gate is closed. This can be done if the univibrator period is extended to a duration longer than the time corresponding to a half-revolution.

The foregoing considerations suggest the desirability of a panel control that permits one to determine the gating period. This feature has not yet been included, but it will probably be incorporated at some future time.

A panel control of gate length offers advantages that can be extended to split-beam operation also. For example, scattered light pulses from the cells sometimes appear with the scanner positioned at a radius-marker hole. A variety of conditions, such as speed and sample content, among others, make it desirable to have control over the channel through which the spurious pulses pass. With split-beam operation it is generally desirable to route the spurious pulses through the reference gate (a 400-μsec one-shot). This is because the reference-cell pulses must activate the switching circuits, and therefore they have appreciable magnitude through most of the scanning period. This being the case, the reference-hold circuit charges to high amplitudes most of the time. The decaying voltage is comparatively large at one-half revolution later when the spurious pulse arrives, and so the holding circuit does not respond (see Fig. 15(b). The spurious pulses, therefore, do not change the output level even though they are permitted to pass through the reference gate.

VIII. PERFORMANCE

A number of performance tests were conducted. Many of these involved oscilloscope presentations, some of which were photographed in order to convey performance characteristics more accurately. Pulse separation, for example, is a major concern, and so a photographic series is included to reveal its effectiveness. Other photographs disclose switching relationships, holding-circuit performance, and logarithmic response. Also included are representative Visicorder tracings, and a calibration plot to indicate the range over which the system is linearly responsive to sample optical density.

With regard to Visicorder tracings, Fig. 17 is an interesting demonstration of performance in each of three modes. Figure 17(a) shows the trace resulting with the Mode switch in Reference position. The reference cell is filled with the solvent (0.1 molar phosphate buffer, pH 7.4), yielding a profile that is flat except for modifications introduced by the system optics. The cell windows have negligible attenuation, and so the downward slope is not attributed to changes in window transmittance. The radius markers appear for reasons described earlier. The upper trace is the derivative; the recorded amplitude is several per cent of the value resulting at maximum gain.

Figure 17(b) shows the trace resulting when scanning the same images with the Mode switch in Sample position. The system now responds to the sample cell contents (alcohol dehydrogenase + DPNH + solvent). This trace is also modified by the system optics. The radius markers are rejected by the gating circuits, as indicated.

The derivative appears to be inverted in the Sample mode. This is due to a reversal of the function galvanometer, normally switched in order to maintain a consistent presentation. The derivative galvanometer is not reversed since the Sample mode is only a cross-check of system performance.

Figure 17(c) records the difference between the first two traces. Radius-marker amplitudes have no significance in terms of density; their principal purpose is to determine the magnification factor of the system. The sharp spike following the left-hand radius marker results from a disparity between the radial positions of the reference and sample cells. The spike adjacent to the right-hand radius marker results from sedimentation in the sample cell. The absorption is high at the outer boundary, and so sedimentation causes the sample cell to appear considerably shorter than the reference cell. The

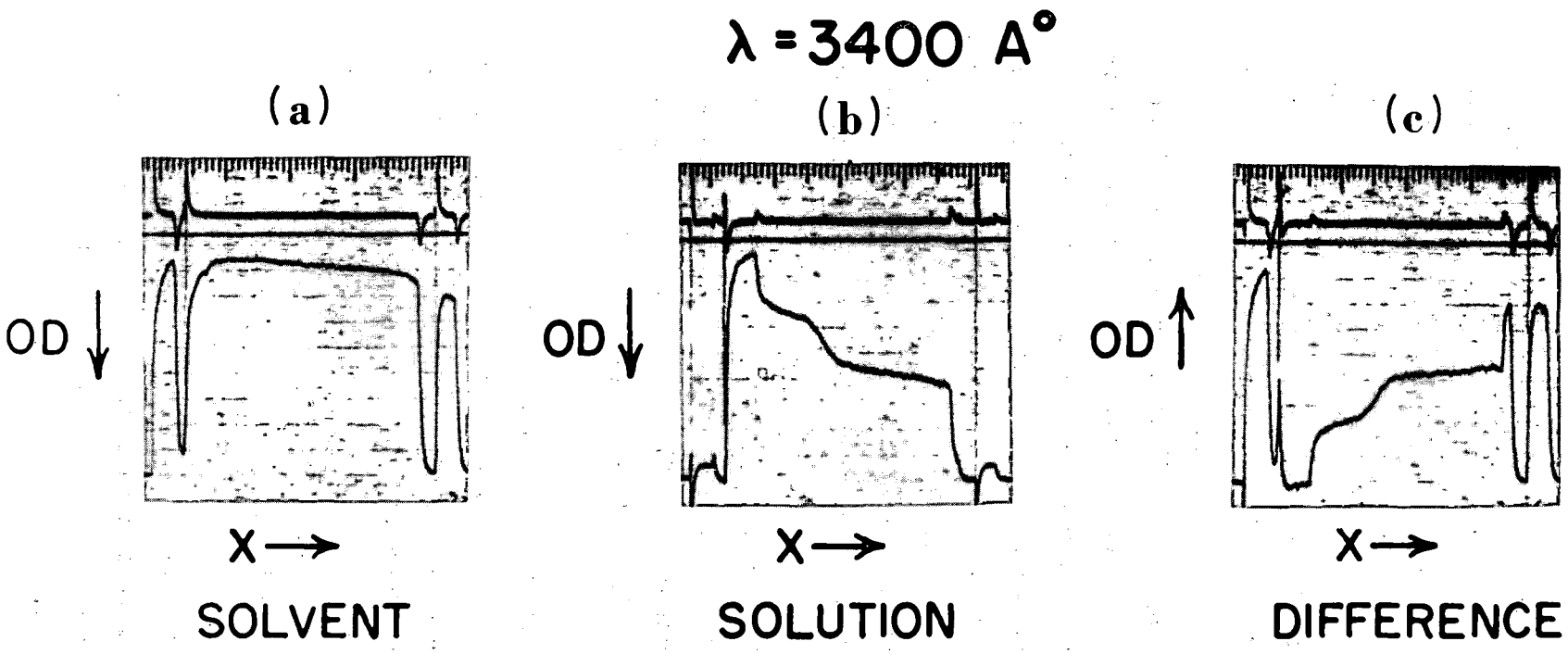

Fig. 17. Visicorder tracings to illustrate operation in each of three modes. The response is logarithmic, and therefore indicates optical density as shown: (a) A scan recorded with the Mode switch in Reference position. The system responds to reference cell content, a solvent (0.1 molar phosphate buffer, pH 7.4). The upper trace records the derivative. (b) A repeat scan with the Mode switch in Sample position. The system now responds to sample cell content, alcohol dehydrogenase plus DPNH dissolved in the solvent indicated above. The radius markers are rejected by the gating circuits. The derivative is inverted for reasons described in the text. (c) A third scan with the Mode switch in Difference position. The system responds to the density difference between cells, compensating for non-uniform illumination. Radius-marker amplitudes have no significance in terms of optical density. The sharp spike following the left-hand radius marker results from a disparity between the radial position of the reference and sample cells. The spike adjacent to the right-hand radius-marker results from sedimentation in the sample cell.

Difference position is the conventional mode when operating split-beam, and the derivative display assumes the correct polarity as indicated.

Another Visicorder series, Fig. 18, records an experiment in which the light source was on the verge of failing, pulsing in amplitude almost periodically. The light fluctuations are especially apparent in Fig. 18(a), taken with the Mode switch in Reference Transmittance position. The series was completed with the Mode switch in Reference (Fig. 18(b), Sample, (Fig. 18(c), and Difference (Fig. 18(d) positions as indicated. The latter responses are logarithmic, and so the light fluctuations are minimized. The pulsations cancel in the Difference mode, excluding radius markers which are expected to fluctuate. Two recordings were taken in the Difference position. One of these, Fig. 18(e) is an expanded version; i. e., the gain has been advanced considerably, moving the upper portion of the radius markers completely off the recording paper.

An examination of Fig. 18 reveals that the resolution is much better than that of the previous series, shown in Fig. 17. This is especially apparent in the menisci and other regions of high density gradient. It should be pointed out that the principal difference between the two series is in the scanning rate. Elaborating, the tracings of Fig. 17 were taken when scanning the images in only 6 seconds. Those of Fig. 18 were recorded when scanning much slower, at 35 seconds. The Visicorder chart speed was adapted accordingly, and so the magnification factor for each series is approximately the same. The system frequency response, determined by the setting of Filter control, was the same in both cases. The faster scanning rates, however, translate a given density gradient into a higher frequency, one that may be limited by system response.

If we wish to scan faster, one alternative is to change the Filter setting, increasing the high-frequency response accordingly. The system is more susceptible to holding-circuit ripple and photomultiplier noise, but measures may sometimes be taken to counter each of these. Ripple, for example, can sometimes be reduced if centrifuge speed is increased. Photomultiplier noise can be reduced by increasing the illumination. This reduces statistical variations to a smaller percentage of the mean value.

Another Visicorder series (Fig. 19) illustrates the compensation resulting from split-beam operation when the illumination is extremely nonuniform. Both cells were empty, offering negligible attenuation, and so the

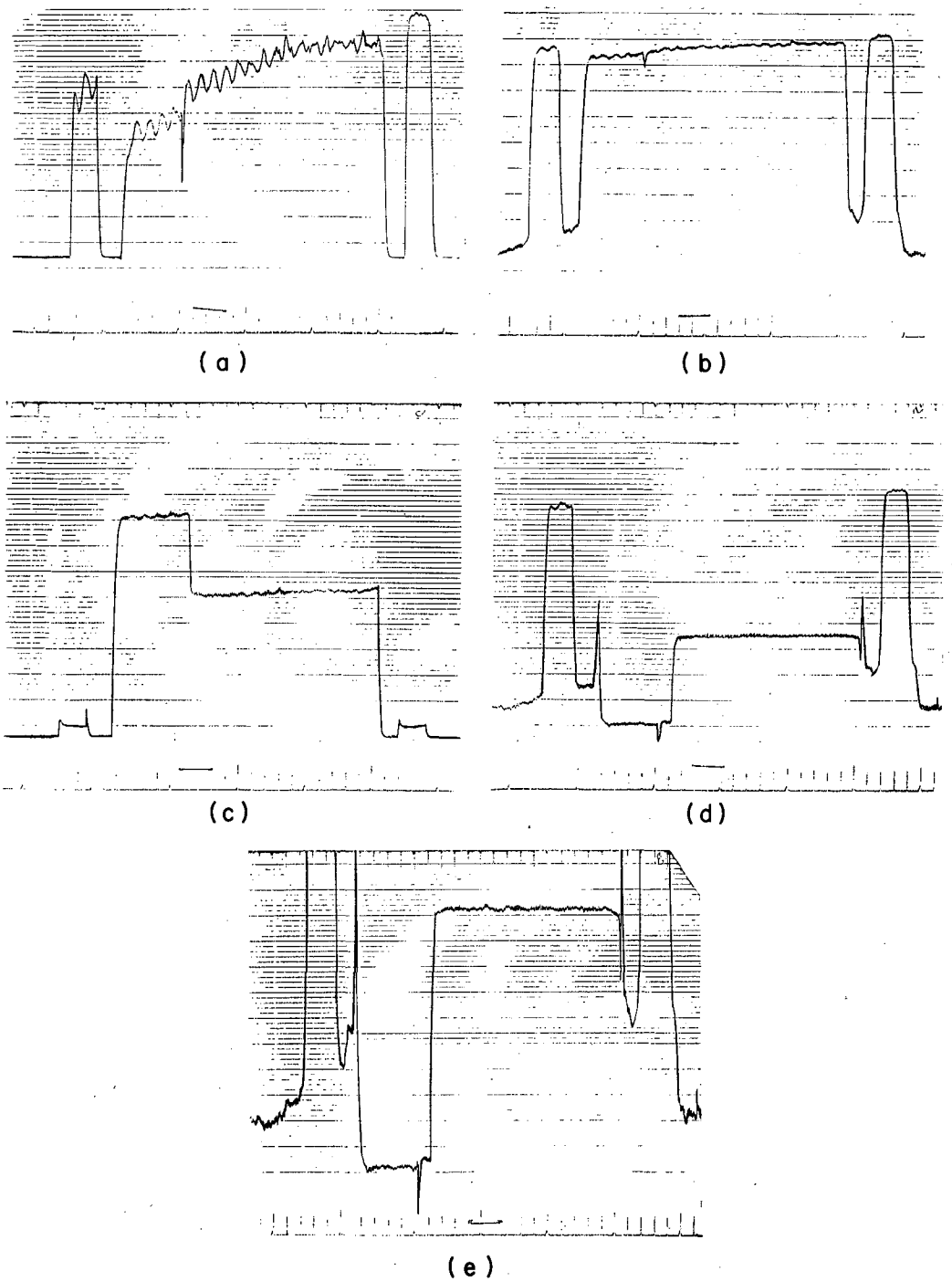

Fig. 18. Visicorder tracings recording an experiment in which the light source was on the verge of failure, pulsing in amplitude, almost periodically:
(a) A scan recorded with the Mode switch in Reference Transmittance. This is a linear response to reference cell content. (b) A repeat scan with the Mode switch in Reference position. Response is logarithmic, and so the fluctuations are less apparent. (c) A third scan with the Mode switch in Sample position. (d) A fourth scan with the Mode switch in Difference. The light pulsations cancel, excluding radius-markers which are expected to fluctuate. (e) An expanded version of (d). The Trace Amplitude has been advanced considerably, moving the upper portion of the radius markers completely off the paper.

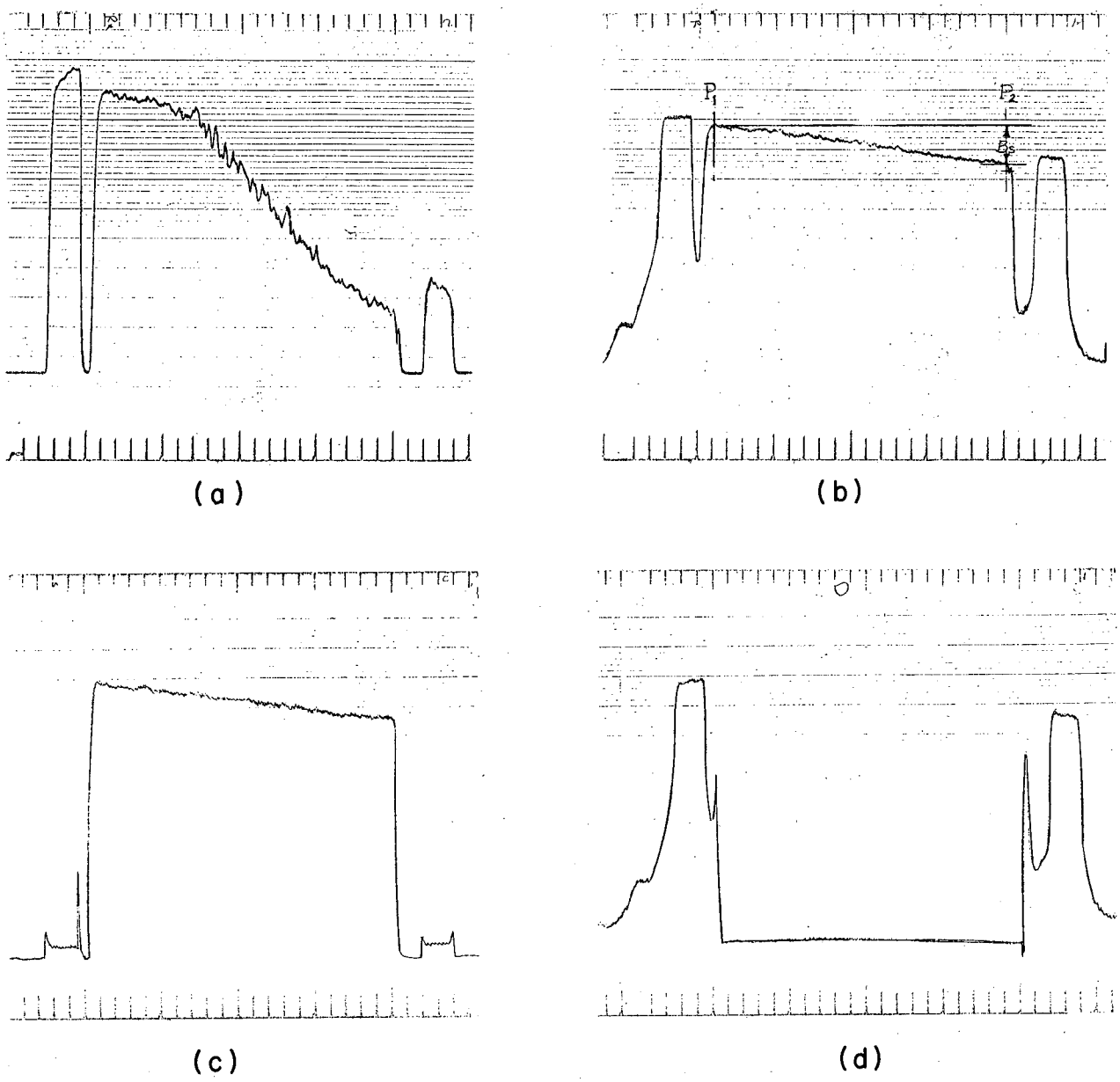

Fig. 19. Visicorder tracings illustrating the compensation resulting from split-beam operation when the illumination is extremely non-uniform. Both cells were empty. B_s shows the baseline shift between scanner positions P1 and P2: (a) Mode switch in Reference Transmittance. A linear recording to emphasize the degree of non-uniformity. (b) Mode switch in Reference. This is a log response to the reference cell. (c) Mode switch in Sample position. (d) Mode switch in Difference position.

reference and sample cell profiles are practically identical. The difference trace shows that the illumination profile is cancelled out, and the baseline is very flat.

The pulse-separation photographs at 60 000 rpm are shown in Fig. 20. The upper circle is a single exposure of an oscilloscope trace, dual-beam. Figure 20(a), upper trace, shows a photomultiplier pulse-pair as it appears at the output of the log amplifier. The lower trace shows the reference-hold response to the same pulse-pair. It will be noted that the reference holding circuit charges to the peak amplitude of the first input pulse. The lower exposure, Fig. 20(b), shows the sample-hold response to the same pair of input pulses. A comparison of exposures reveals that the pulses are effectively separated, and that each of the two "mates" is routed to the appropriate holding circuit.

The sample-hold response to a single pulse-pair is shown in Fig. 20(b). The response to consecutive pulse-pairs can be observed if the oscilloscope sweep speed is reduced, as shown in Fig. 21. The time separation between "mates" is very small as compared to the time per revolution, and so it is somewhat difficult to detect that the pulses come in pairs. Zero output from the holding circuit corresponds to the bottom line of the reticle. The sample-hold output, lower trace, shows that the decay time constant is very effective in increasing the average output voltage. With the time constant shown, a representative value, the average output level is approximately 75% of the peak input voltage. This is an appreciable factor over an estimated 0.5% expected from a low-pass filter of the type employed by the previous, single-beam system.

With regard to switching, the gating circuits have been very reliable in practice, and it is possible to cover the speed range between 1000 and 60 000 rpm without changing the Delay control. It is generally adequate to set the control to a predetermined dial setting, no further adjustment being required.

In order to have reliable switching the reference pulse amplitude must be at least 0.8 V when measured at the photomultiplier output. At some centrifuge speeds the reference cell meniscus offers appreciable attenuation, and so synchronization is disrupted while scanning that meniscus. This diverts the sample pulses through the reference gate, leaving a sharp void in the sample

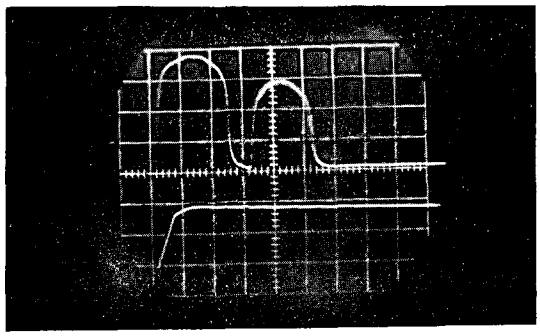

(a)

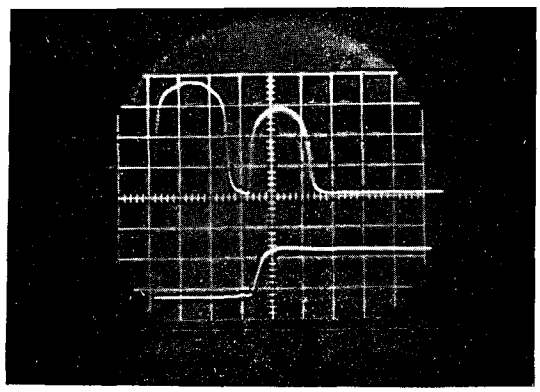

(b)

ZN-3604

Fig. 20. Pulse-separation photographs at 60 000 rpm. Each circle is a single exposure of an oscilloscope trace, dual-beam: (a) The upper trace shows a photomultiplier pulse-pair as it appears at the output of the log amplifier. The trace beneath it shows the voltage across the reference hold circuit. (b) Shows the sample hold response to the same pair of input pulses. Comparison of (a) and (b) shows the pulses effectively separated, and that each of the two "mates" is routed to the appropriate holding circuit.

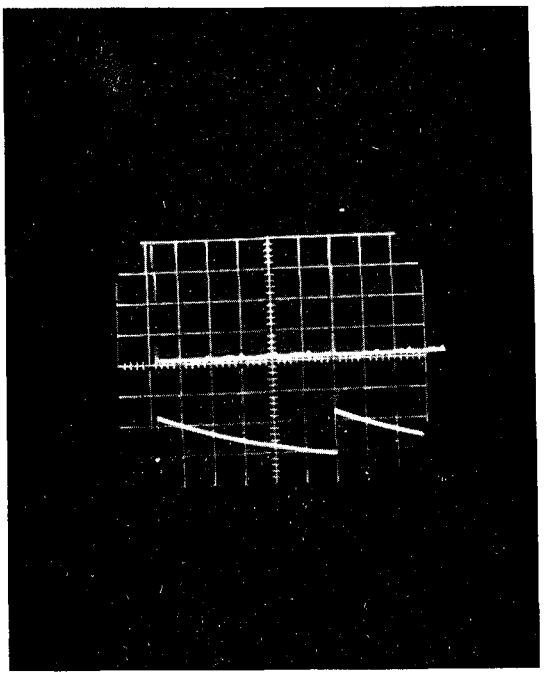

ZN-3602

Fig. 21. This is a repeat of Fig. 20(b), excepting oscilloscope sweep speed. The speed has been reduced enough to show the sample-hold response to two sets of pulse-pairs. The time separation between "mates" is very small when compared to the time per revolution, so it is difficult to detect the pulse-pairs which are very prominent in Fig. 20(b).

profile. The reference meniscus is reflected in the sample channel, but performance is not impaired over the remaining portion of the scan. The meniscus occupies a very small percentage of the total image length, however, and so the effect is not deleterious. It should be pointed out that this is an anomalous condition; i.e., the reference-pulse amplitude when scanning the meniscus is generally adequate to maintain synchronization.

The switching time measures less than 1 μsec, as shown in Fig. 22, which is a single exposure of a dual-beam trace. The upper trace shows a photomultiplier pulse pair; the lower trace is the switching signal measured at the blue test point of Fig. 5. This photograph confirms that switching occurs in the time interval between "mates."

Referring to Fig. 5, we see that the switching signals applied to the reference and sample gates are out of phase. The actual waveforms are recorded in Fig. 23. The upper circle shows the switching signal applied to the reference gate (blue test point); the lower exposure indicates the switching signal to the sample gate (purple test point). Each gate is open when the applied waveform is negative. Figure 23 indicates that the sample gate is open to transmission for 440 μsec, the measured duration of the one-shot pulse. The reference gate is then opened, permitting transmission until the trailing edge of the first pulse from the next "pair" arrives (720 μsec at the speed indicated). To summarize: the sample gate is open for a fixed period of time. The duration does not change with speed, and it is determined by the one-shot. The reference "gate-open" period, on the other hand, is subject to centrifuge speed. The reference gate is open for a period equal to the time required for the rotor to make one revolution, minus the gating length of the one-shot.

Also interesting is the time required for the holding circuits to charge up to a given percentage of the input signal level. This is related to the Holding Capacitor selector switch setting, calibrated in terms of speed. When the Holding Capacitor switch is set for the 60 000-rpm range, the sample-hold charging time measures 2 μsec, as shown in Fig. 24 (lower trace). The photograph is a single exposure, dual-trace, showing the sample-hold response with the Mode switch in Reference position and with a 6 V battery connected to the input (pin 9) of the sample gate. When so operated, none of the pulses is applied to the sample gate input. The sample-hold circuit now responds to the 6 V battery, which is alternately connected and disconnected by the switching circuits.

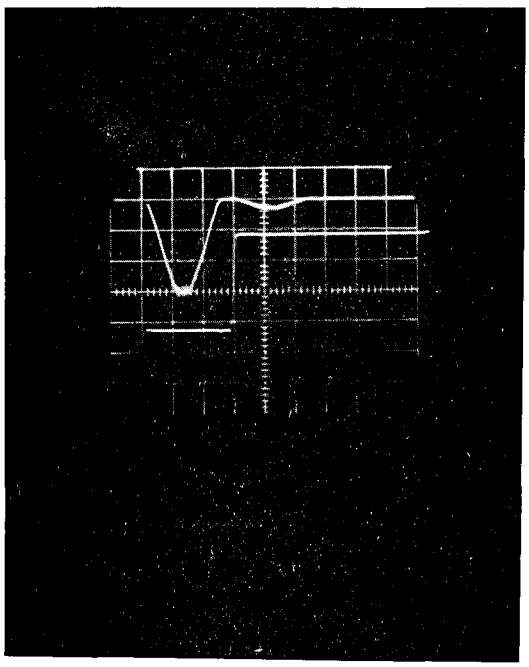

ZN-3603

Fig. 22. Switching photographs at 60 000 rpm, a single exposure of a dual-beam trace. The upper trace shows a photomultiplier pulse-pair; the lower trace is the switching signal measured at the blue test point of Fig. 5. The sweep speed is 5μsec/cm, indicating that the switching time measures less than 1μsec. This photograph also confirms that switching occurs in the time interval between "mates."

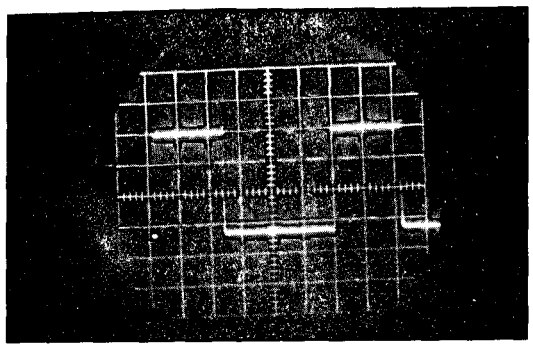

(a)

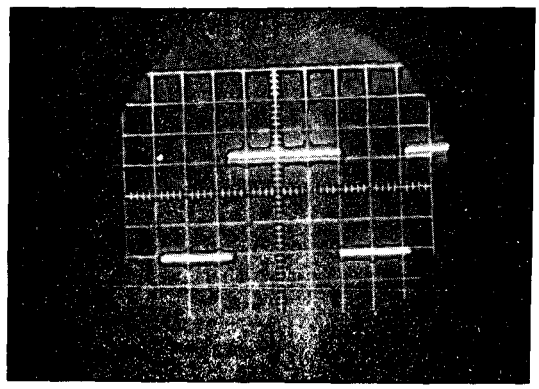

(b)

ZN-3607

Fig. 23. Photographs which show the switching signals applied to reference and sample gates. The oscilloscope sweep speed is 200 μsec/cm. The vertical sensitivity is 10V/cm, and zero volts corresponds to the centerline of the reticle. Each gate is open when the applied waveform is negative. (a) Shows the switching signal applied to the reference gate (blue test point). The reference gate is open to transmission for 720 μsec at the centrifuge speed indicated. (b) The switching signal applied to the sample gate (purple test point). The sample gate is open for 440 μsec, the measured duration of the one-shot pulse.

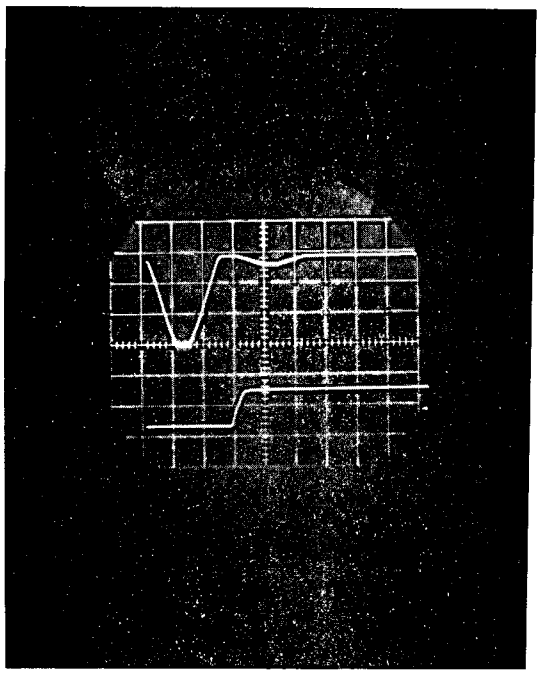

ZN-3601

Fig. 24. A single exposure, dual-trace, for measuring the sample-hold charging time at 60 000 rpm. The upper trace shows a photomultiplier pulse-pair. The lower trace indicates the sample-hold voltage with the Mode switch in Reference position and with a 6-V battery connected to the input (pin 9) of the sample gate. When so operated, none of the pulses is applied to the sample gate input. The sample-hold responds to the 6-V battery, alternately connected and disconnected by the switching circuits. The sweep speed is 5 μsec/cm. The charging time measures 2 μsec, with the Holding Capacitor set for the 60 000-rpm range.

Another concern is the logarithmic response to pulses, especially at 60 000 rpm. With this in mind, another series of photos was taken to test the frequency and amplitude characteristics of the log amplifier. One photograph, Fig. 25 (lower trace), shows the log amplifier response to a photomultiplier pulse-pair (upper trace). The waveform is clean, and the pulse-amplitude ratio conforms to the value expected from the manufacturers data on the log compressor (Fig. 26).

The system response to pulse amplitude is also important. With this in mind, Visicorder deflection vs reference pulse amplitude is plotted on semilog paper, as shown in Fig. 27. Data were taken with the scanner positioned at one of the radius markers. The Mode switch was in Reference position, and the switching circuits were disabled by turning the Delay control completely clockwise to eliminate switching as a source of error. The photomultiplier voltage was adjusted to produce reference pulses of various heights and the Visicorder deflection recorded. The resulting plot indicates that the response is logarithmic over an extended range. Subsequent tests revealed that the nonlinearity at the higher input levels may be attributed to the log compressor. The plot does not pass through the origin because the charging diode requires a fractional volt in order to become conductive.

Future requirements indicate that it will be desirable to add a closed-loop system for regulating the reference-pulse amplitude. Such a scheme would control photomultiplier voltage, influencing reference and sample pulses proportionately. Regulation ensures that operation is always confined to the most desirable region of the log amplifier, and that none of the linear region is "wasted" in compensating for non-uniform illumination.

The last, but not the least consideration, is the system response to solutions of measured optical densities. This is shown by the calibration plot of Fig. 28. This is a measure of total response, and indicates that the system is linearly responsive (accuracy ± 2% of full-scale deflection) to optical densities between zero and 1.8.

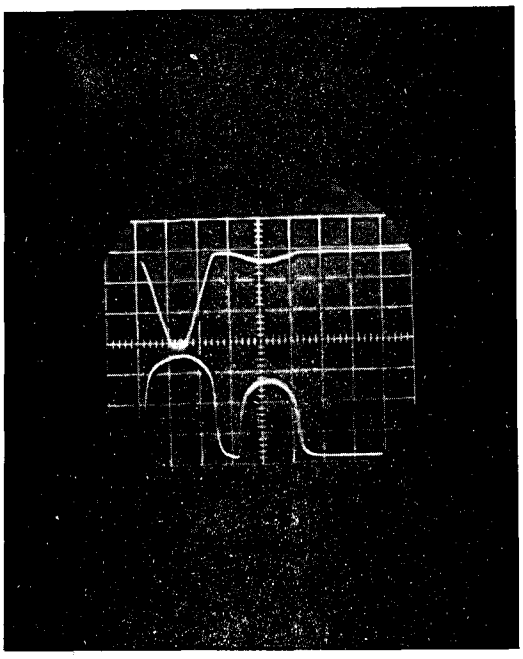

ZN-3600

Fig. 25. A single exposure, dual-trace, showing the log amplifier response to a photomultiplier pulse-pair at 60 000 rpm. The sweep speed is 5 μsec/cm. The output waveform from the log amplifier is indicated by the lower trace.

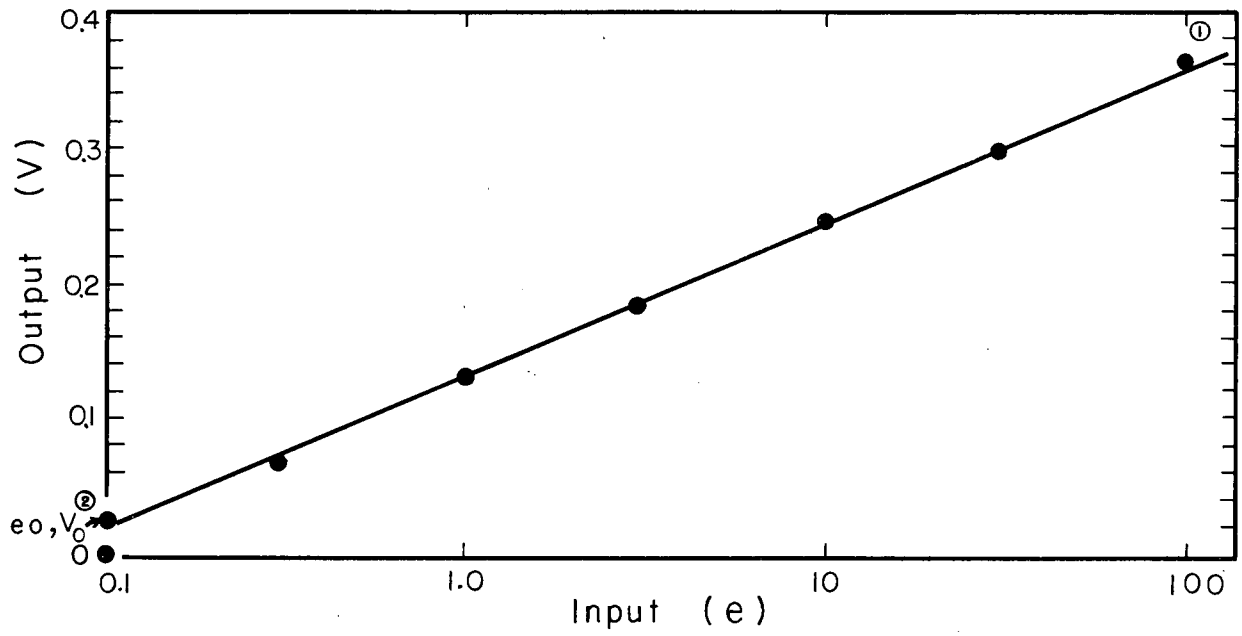

Fig. 26. Logarithmic compressor amplitude response, manufacturers data. Test points are at 1 kc. Model C-7A logarithmic voltage compressor (Kane Engineering Laboratories, Palo Alto, California).

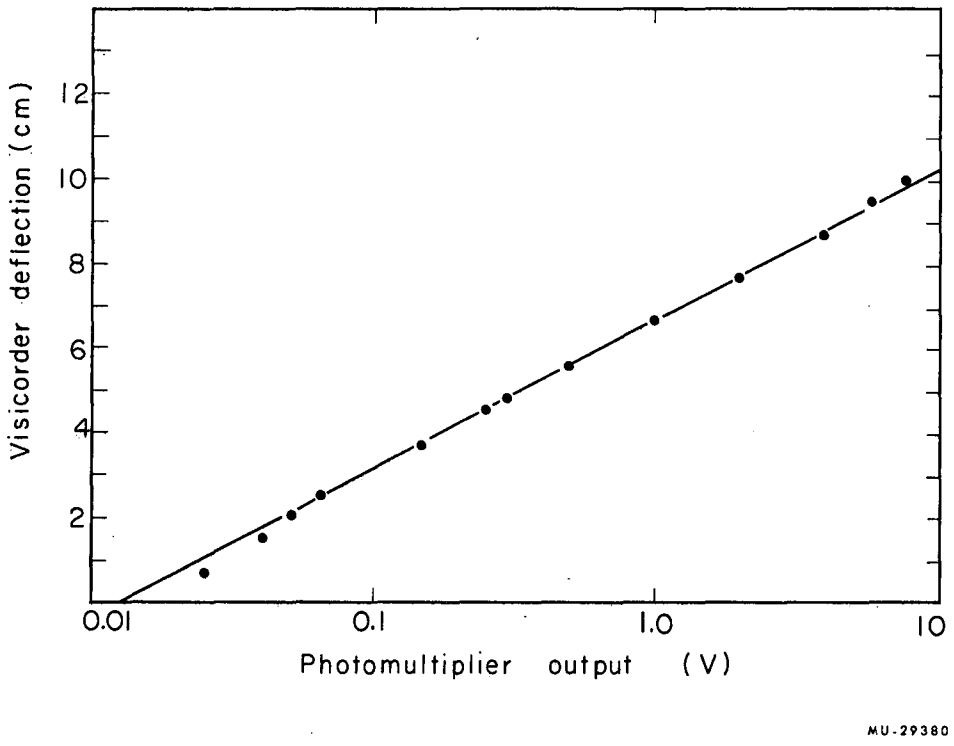

Fig. 27. Visicorder deflection vs reference pulse amplitude, Mode switch in Reference position, and the switching circuits disabled with the delay control. The scanner was positioned at a radius-marker and the photomultiplier voltage adjusted to produce pulses of various heights.

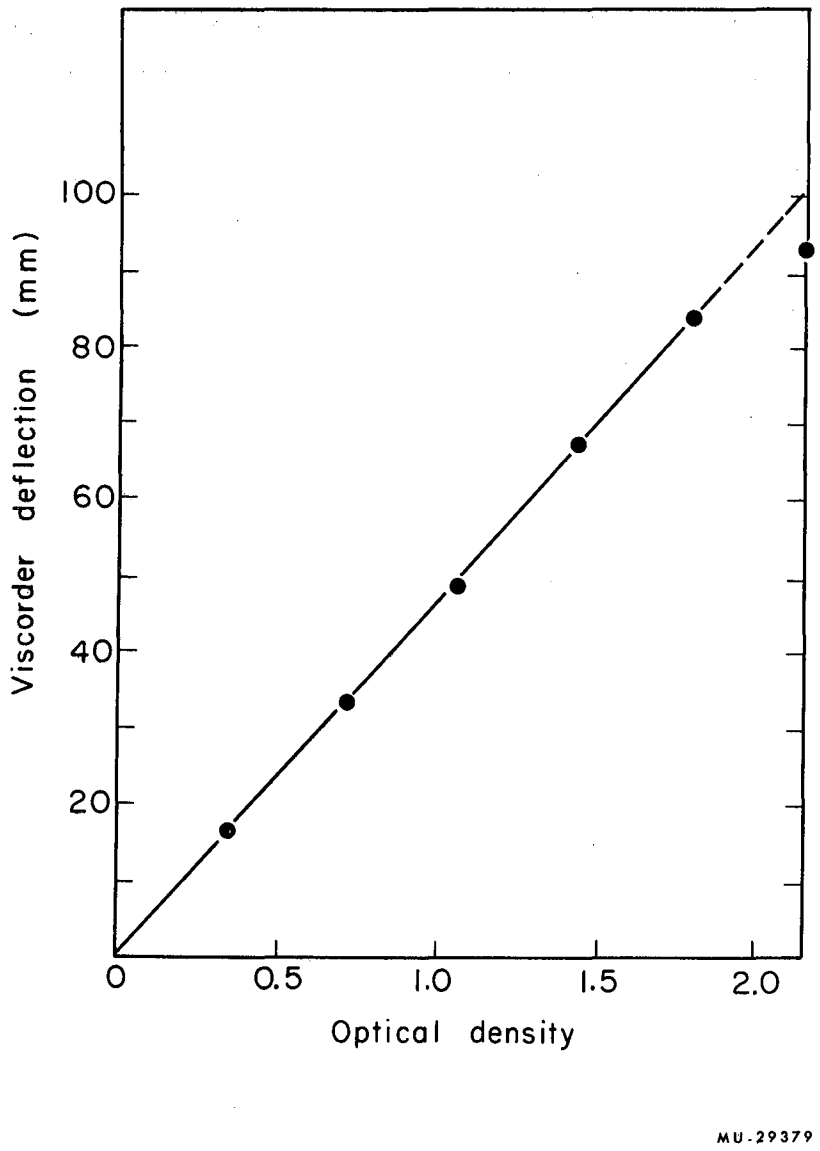

Fig. 28. System response to solutions of measured optical densities, Mode switch in Difference position. The deflections indicated are approximately 20% of those obtainable at maximum gain. The calibration indicates that the system is linearly responsive (accuracy ±2% of full-scale deflection) to optical densities between zero and 1.8. The photomultiplier voltage was adjusted for 2-V reference pulses at the air space.

ACKNOWLEDGMENTS

The photoelectric scanner design was sponsored by Professor Howard K. Schachman of the Biochemistry and Virus Laboratory, University of California at Berkeley. He also conceived the split-beam application to centrifuge work, and is responsible for most of the optics relevant to the transition from photographic recording. The scanning mechanism was designed by Messrs. F. Bierlein, R. Johnson, G. Lauterbach, and F. Plunder. Mr. Paul Strom assisted with the electronic circuitry. The initial manuscript was read by Mr. Charles G. Dols, who was consulted throughout the work and provided useful design suggestions.

APPENDICES

A. Derivations

The primary requirement of any system is that its response be linearly related to the optical density OD of the sample, or by definition,

$$OD = \log I_o/I, \tag{1}$$

where OD is the optical density of the sample, I_o is the light intensity entering the sample, and I is the attenuated value after absorption.

The ratio I/I_o is termed transmittance. With regard to the sample, the term I/I_o may be designated ν, or:

$$\nu = I/I_o. \tag{2}$$

Substituting (2) into (1) we obtain

$$OD = \log 1/\nu . \tag{3}$$

The next procedure is to develop an expression for the system response in order to ascertain that it does conform to Eq. (3). With this in mind a derivation follows:

Figure 29(a) is a simplified diagram of the reference-cell optics, consisting of a light source, the reference cell, and a photomultiplier. If we assume that the photomultiplier is linearly responsive to light intensity, it develops a peak pulse amplitude proportional to its sensitivity P_r, the light intensity L_r, the light-fraction intercepted f_r, and the transmittance of the reference cell R (cell window plus solvent). Expressed as an equation, this gives us

$$e_r = P_r L_r f_r R \qquad (e_r = \text{PM output voltage}). \tag{4}$$

Referring to Fig. 29(b) the sample path includes the sample cell of transmittance S (cell window plus solvent) and a virus[12] concentration of transmittance ν:

$$e_s = P_s L_s f_s S \nu \tag{5}$$

The subscripts to P, L, and f have been introduced to account for differences between each channel. If the time interval between sample and reference pulses is short, and if the scanning mechanism moves only a short distance during that time, the ratios P_r/P_s, L_r/L_s, and f_r/f_s can be considered to be 1. Their individual values may vary throughout the scan, but their ratios do not.

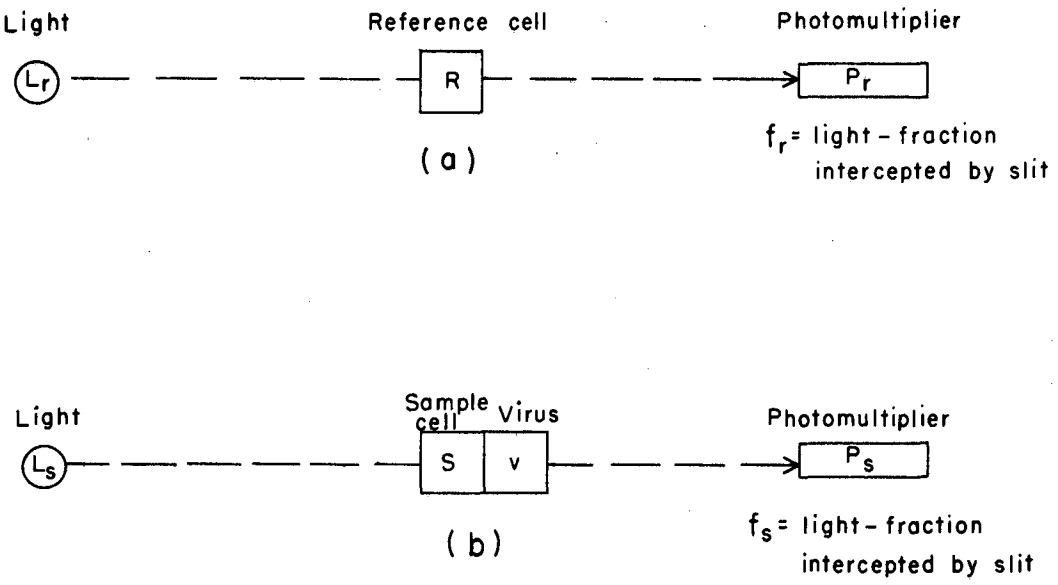

Fig. 29. Optical system, simplified diagram, for purposes of derivation: (a) Reference-cell light path, and (b) Sample-cell light path.

If we take the log of Eqs. (4) and (5), and then subtract,

$$\log e_r - \log e_s = \log R/S - \log \nu \, . \qquad (6)$$

If the ratio R/S is constant, Eq. (6) indicates that the log difference varies with virus density, and that it is displaced from zero by some amount related to the ratio R/S. If R/S is 1, there is no displacement, and the output level is directly proportional to virus optical density.

The preceding discussion indicates that a log operation is necessary, but does not provide for the fact that the log amplifier is logarithmic over a limited range. It also fails to consider channel disparities, such as channel gain differences. With this in mind, a derivation involving the additional parameters follows:

Referring to Fig. 5, we find that each channel produces a holding circuit voltage H proportional to the log-amplifier output voltage V, channel gain A, and holding-circuit gain constant T. Writing the expression for each channel, we obtain

$$H_r = V_r A_r T_r \, , \qquad (7)$$

and

$$H_s = V_s A_s T_s \, . \qquad (8)$$

Let us assume that the log amplifier is common to both channels, that its response is similar to that shown in Fig. 26, and that operation is confined to the linear region between 1 and 2. An examination of the figure reveals that the peak pulse amplitude appearing at the log amplifier output may be described by an equation of the form, $V = V_0 + m(\log e - \log e_0)$. Elaborating, the log output voltage V is equal to some constant V_0, plus the slope m, (which depends upon log-amplifier gain), times the difference between the logs of the input voltage e and the voltage corresponding to the abscissa of V_0, or e_0. Expressed as an equation for each channel, we have

$$V_r = V_0 + m(\log e_r - \log e_0), \qquad (9)$$

and

$$V_s = V_0 + m(\log e_s - \log e_0) \, . \qquad (10)$$

In practice, the log output voltage from each channel is routed to a different holding circuit, and so the gain constants T_r and T_s are not exactly equal. This is corrected with the Null adjustment so that the gain ratio A_r/A_s compensates for their difference.

Substituting the values of (9) and (10) into (7) and (8) respectively, the holding circuit voltages, H, may be expressed

$$H_r = A_r T_r (V_0 + m \log e_r/e_0) \qquad (11)$$

$$H_s = A_s T_s (V_0 + m \log e_s/e_0). \qquad (12)$$

With regard to recorder deflection D, the amplitude is proportional to the voltage difference across the holding circuits multiplied by the gain constant G that follows the difference amplifier input. Rewriting and substituting the values of Eqs. (11) and (12), we get

$$D = G\left[A_r T_r (V_0 + m \log e_r/e_0) - A_s T_s (V_0 + m \log e_s/e_0)\right]. \qquad (13)$$

The null adjustment is normally made in the air space where the transmittance ν is equal to 1. When D is adjusted for zero, the gain ratio has been adjusted so that

$$A_r T_r = A_s T_s \left[\frac{V_0 + m \log e'_s/e_0}{V_0 + m \log e'_r/e_0}\right]. \qquad (14)$$

The primes have been added to represent the photomultiplier output voltages when positioned in the air space at both cells ($\nu = 1$).

If Eqs. (4) and (5) are substituted into Eq. (14), and if it is assumed that the quantities, P, L, and f, do not change in the time interval between the reference and sample pulses, and that the values of R and S are equal and constant, then

$$A_r T_r = A_s T_s . \qquad (15)$$

Substituting the values of Eqs. (4), (5), and (15) into Eq. (13), the recorder deflection D becomes

$$D = G A_s T_s m \log 1/\nu . \qquad (16)$$

Equation (16) indicates that the recorder deflection is proportional to virus concentration. The amount of deflection for a given virus transmittance is controlled by adjusting the value of G. This is done with an adjustable attenuator (Trace Amplitude), which determines the output level applied to the Visicorder galvanometer. This equation also indicates that the system response is independent of variations appearing in the illumination profile.

The previous derivation was made on the assumption that R and S are equal. Equation (16) shows that non-uniform illumination is not important, provided that we stay within the linear region of Fig. 26. Let us now assume that R and S are not equal, then deduce the errors resulting from non-uniform illumination profiles that are considered acceptable to system performance.

Substituting Eq. (14) into Eq. (13), we have

$$D = G A_s T_s \left[\left(\frac{V_0 + m \log e_s'/e_0}{V_0 + m \log e_r'/e_0} \right) (V_0 + m \log e_r/e_0) - (V_0 + m \log e_s/e_0) \right] . \tag{17}$$

The quantity in the first parentheses is a constant K_1. Referring to Eq. (14), it represents the ratio $A_r T_r / A_s T_s$ after the null adjustment has been made. Its exact value depends upon the absolute magnitudes of P, L, and f which existed at the time of nulling, or

$$K_1 = \frac{V_0 + m \log e_s'/e_0}{V_0 + m \log e_r'/e_0} . \tag{18}$$

If we assume that P, L, and f are constant in the time interval between pulses, substituting Eqs. (4), (5), and (18) into Eq. (17):

$$D = G A_s T_s \left[K_1 (V_0 + m \log P L f R/e_0) - (V_0 + m \log P L f S v/e_0) \right] \tag{19}$$

This may be rewritten:

$$D = G A_s T_s \left[K_1 V_0 + K_1 m \log R/e_0 - V_0 - m \log S/e_0 + K_1 m \log P L f - m \log P L f - m \log \nu \right] . \tag{20}$$

The first four terms are constant-if we call K_2

$$K_2 = (K_1 - 1) V_0 + K_1 m \log R/e_0 - m \log S/e_0 . \tag{21}$$

Substituting Eq. (21) into (20), and rewriting, we have

$$D = G A_s T_s \left[K_2 + (K_1 - 1) m \log P L f - m \log \nu \right] . \tag{22}$$

Equation (22) reveals that if R and S are not equal, the virus profile will be modified by the illumination profile. The degree of modification is related to the percentage variation of the quantity (P L f) and to the magnitude of $(K_1 - 1)$. Referring to Eq. (18), when R and S are equal, both pulses, e'_s and e'_r, are equal, and so K_1 is equal to 1. In that case, K_2 and the illumination term, $(K_1 - 1)$ m log P L f, fall out of Eq. (22), as expected.

Let us now consider the practical case to find out the extent to which this split-beam system compensates for non-uniform illumination profiles. The Visicorder tracings of Fig. 19 are a good example. Both cells were empty, offering negligible attenuation, and so the reference and sample cell profiles are practically identical. The difference trace shows that the illumination profile is cancelled out, and so the baseline is very flat. The values of R and S are very closely matched, but this is not surprising since both cells are enclosed by a common window material.

The values of R and S are usally equal, but it is useful when they are not to have an equation formulating the magnitude that the baseline shifts. Referring to Eq. (22), we see that non-uniform illumination produces a baseline shift B_d equal to the change in value of the quantity $G A_s T_s(K_1 - 1)$ m log P L f from the value that it assumes at the position where the null is made. This deviation from the true baseline B_d changes with scanner position, and it may be expressed as

$$B_d = G A_s T_s(K_1 - 1) m (\log P' L' f' - \log P L f), \quad (23)$$

where P', L', and f' represent the magnitudes of P, L, and f at the time when the null adjustment was made.

The absolute magnitude of B_d can be computed, if desired, but there is another quantity related to it which is more interesting. For example, it is useful to know how a baseline shift with the difference system compares with the shift of single-beam, assuming the illumination profile is the same in both cases. Referring again to Fig. 19(b), reference optical density prior to taking the difference, the illumination profile changes by a magnitude B_s when the scanner is moved from P_1 to P_2. This is equivalent to a shift in the baseline, and we wish to know the extent to which the magnitude of B_s is reduced by the difference system when R and S are not equal. In essence, we wish to know the ratio of B_d/B_s.

The magnitude of B_s can be deduced from Eq. (13). When the Mode switch is in Reference position, the holding circuit voltage H_s of Eq. (12) does not appear in the output, and so the deflection in this mode, D_s, becomes

$$D_s = G A_r T_r(V_0 + m \log e_r/e_0). \quad (24)$$

The baseline shift in this mode, B_s, is equal to the difference between the values that D_s assumes when the scanner is moved from position 1 to position 2 of Fig. 19(b). Assuming that the null is made at position 1, substituting Eqs. (4) and (5) into (24), we obtain the value of D_s for positions 1 and 2:

$$D_s 1 = G A_r T_r (V_0 + m \log P' L' f' R/e_0) \text{ (position 1)}, \quad (25)$$

and

$$D_s 2 = G A_r T_r (V_0 + m \log P L f R/e_0) \quad \text{(position 2)}, \quad (26)$$

The baseline shift B_s is equal to the difference between Eqs. (25) and (26). Subtracting and simplifying, we obtain

$$B_s = G A_r T_r m(\log P' L' f'/P L f) \quad (27)$$

Substituting Eq. 14 into 27, we get

$$B_s = G A_s T_s m\left(\frac{V_0 + m \log e_s'/e_0}{V_0 + m \log e_r'/e_0}\right) \log P' L' f'/P L f \quad (28)$$

Substituting Eq. (18) into (28), we have

$$B_s = G A_s T_s m K_1 \log P' L' f'/P L f . \quad (29)$$

We wish to find the ratio B_d/B_s. Substituting the values of Eqs. (23) and (29), and simplifying, we get

$$B_d/B_s = (K_1 - 1)/K_1 . \quad (30)$$

If Eq. (30) is to be of value, we must determine some typical values of K_1. Equation (18) formulates its magnitude, but we need to know the magnitude of m. Referring to Fig. 26 and Eq. (9), and substituting arbitrary values, we have

$$0.36 = 0.02 + m (\log 100 - \log 0.1). \quad (31)$$

Solving for m, we obtain

$$m = 0.11. \quad (32)$$

Referring now to Eq. (18) and Fig. 26, assume a mismatch between the reference and sample pulse voltages. A 20% mismatch would typically represent values of 5 and 6 volts for e'_s and e'_r respectively. Substituting the appropriate values from Fig. 11 into Eq. (18), we obtain

$$K_1 = \frac{0.02 + 0.11 \log 5/0.1}{0.02 + 0.11 \log 6/0.1} = 0.958 . \qquad (33)$$

Substituting the value of K_1 from Eq. (33) into (30), we get

$$B_d/B_s = (0.958 - 1)/0.958 = - 0.0438 . \qquad (34)$$

The negative sign indicates an overcompensation when the value of $e'_s < e'_r$. If their values are interchanged to become 5 V for e'_r and 6 V for e'_s, Eq. (34) assumes a value of +0.041.

Equation (34) indicates that if the cells are mismatched in the ratio of 5/6, the difference system reduces the magnitude of the baseline shift to 4.4% of the value that it would have in the absence of the difference scheme.

B. Schematics for Split-Beam Operational Unit

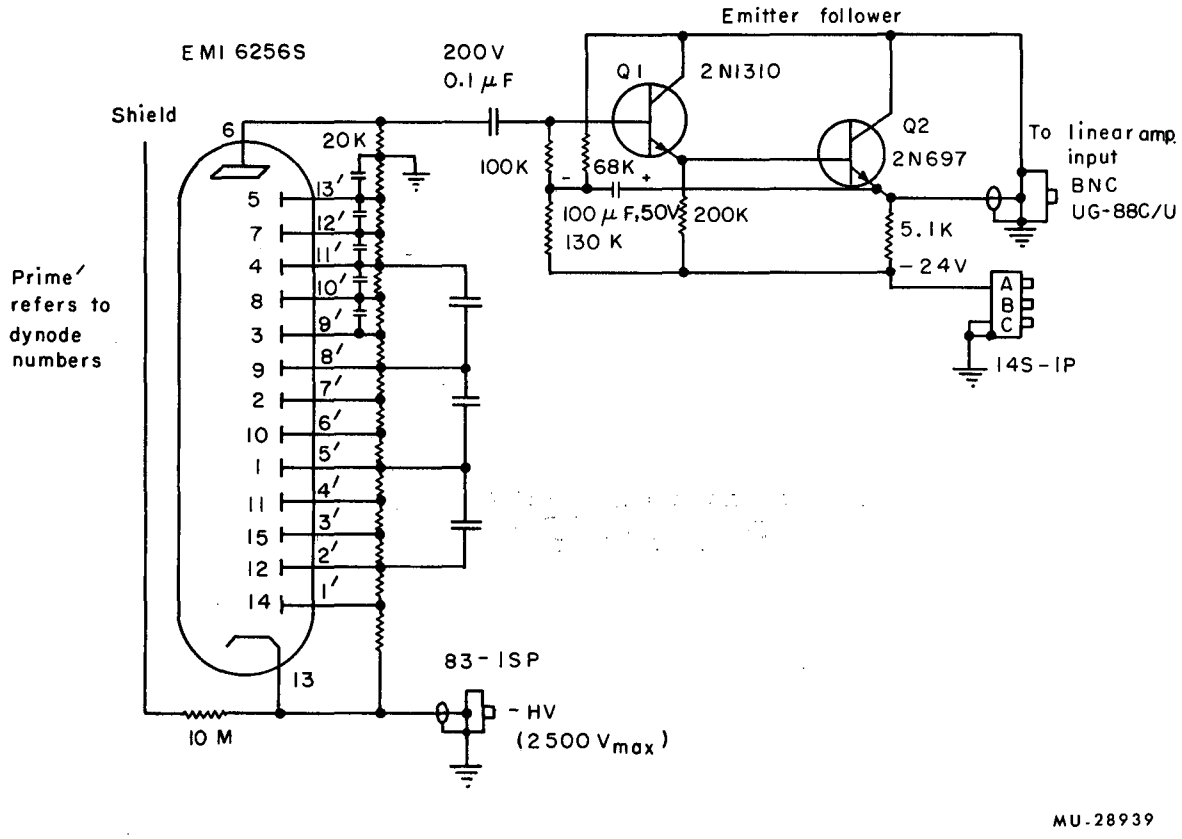

Fig. 30. Photomultiplier and emitter follower. All photomultiplier resistors are 100 k, 0.5 W, 5%, unless otherwise noted. Capacitors are 0.02 μF, 1 kV ceramic. All emitter-follower resistors are 0.5 W.

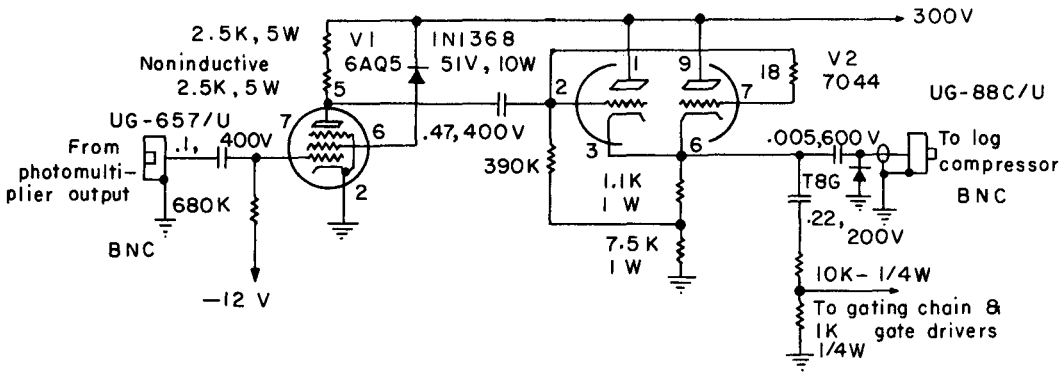

Fig. 31. Linear amplifier. All resistors are 0.5W unless otherwise noted. The orange test point shown in Fig. 5 connects to pin 6 of V2. The red test point connects to the photomultiplier output.

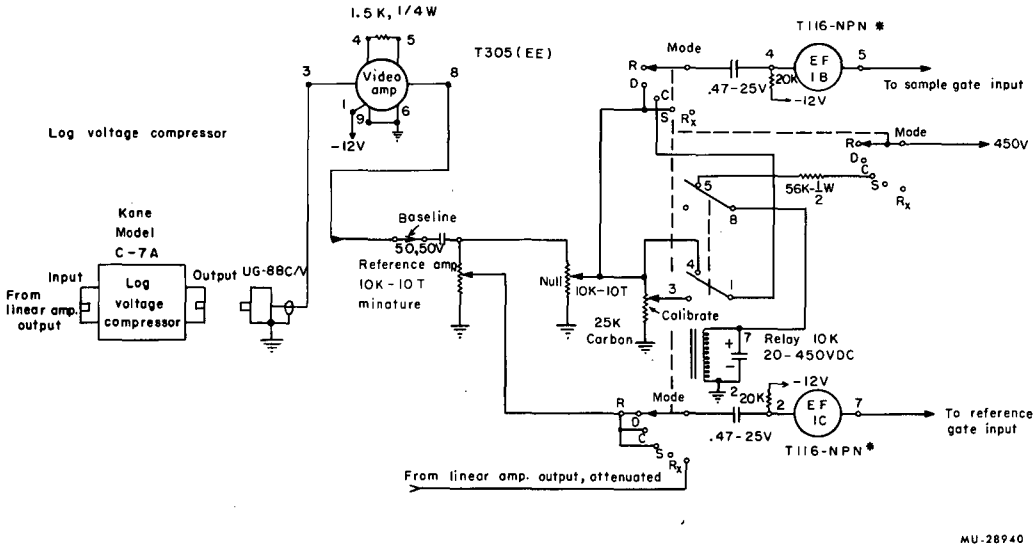

Fig. 32. Log amplifier. All resistors are 0.5 W unless otherwise noted. Asterisk (*) indicates a packaged circuit, Engineered Electronics Company, T-series. Pin 1 connects to -12 V, pins 6 and 9 connect to ground. The log compressor is battery operated as supplied. The batteries are replaced by a power supply.

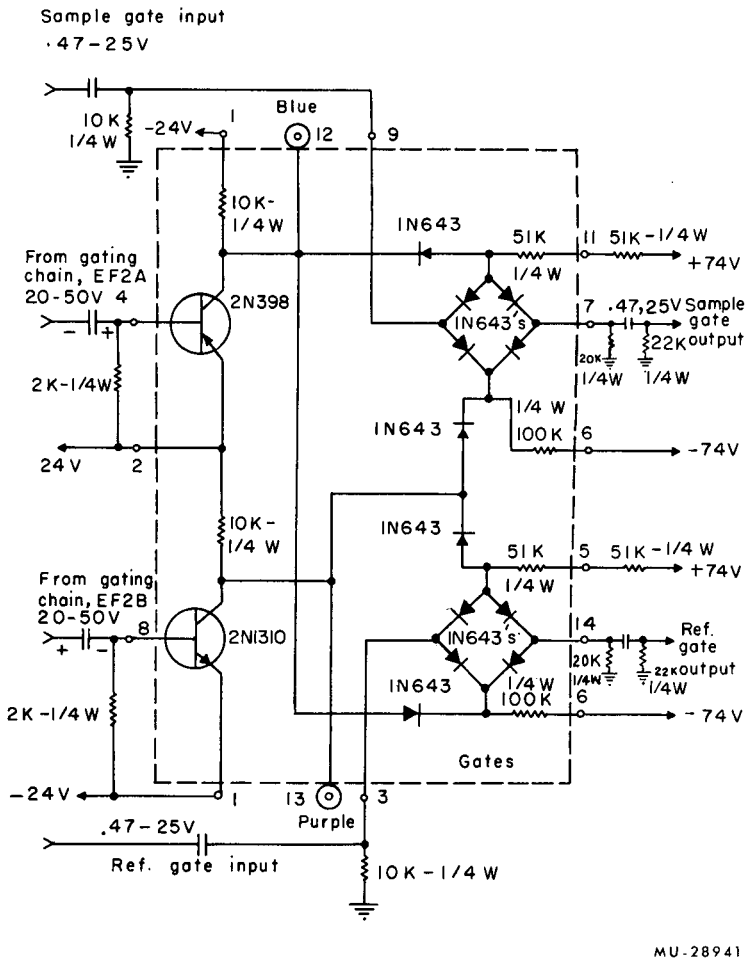

Fig. 33. Switch and 6-diode gates. The reference gate output capacitor is 0.47 μF, 25 V.

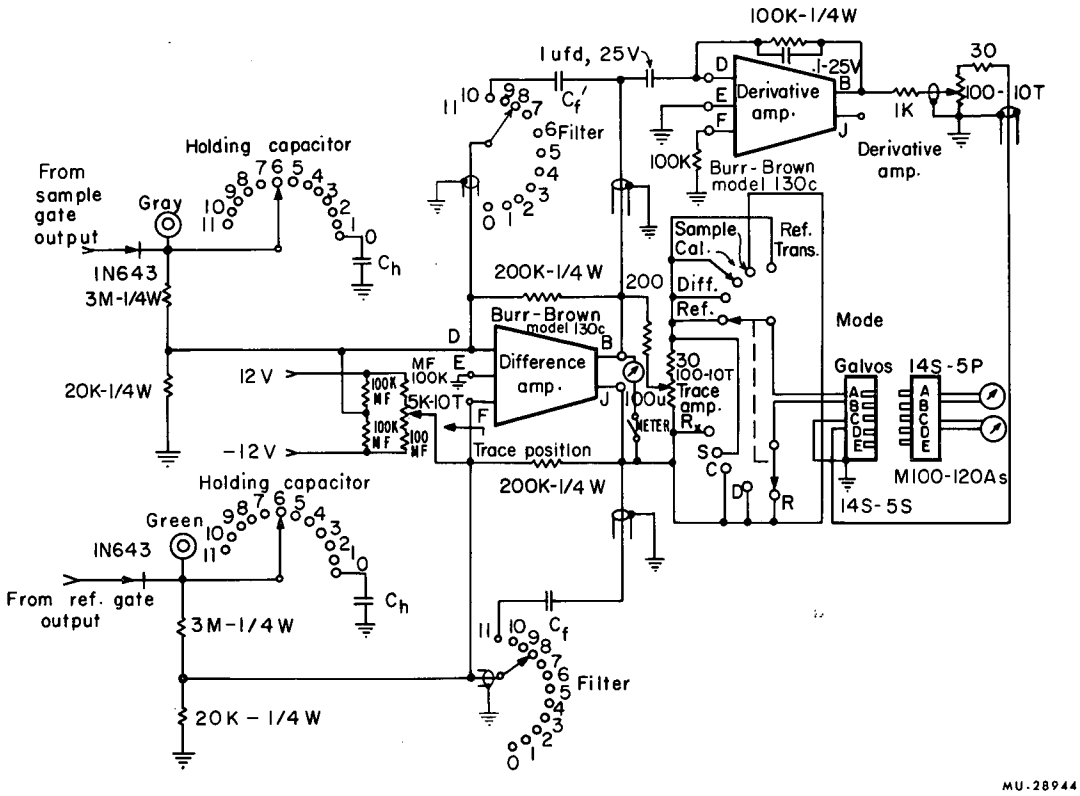

Fig. 34. Holding circuits, difference and derivative amplifiers. All resistors are 0.5 W unless otherwise noted. The Burr-Browns operate with +12 V to pin A and -12 V to pin L. The derivative sensitivity can be increased if the 1-k output resistor is reduced to 200 ohms. The derivative signal-to-noise ratio can be improved by increasing the derivative amplifier feedback capacitor (0.1 μF, 25 V) to a larger value. A switch has been added, permitting one to shunt the 0.1 μF with 0.47 μF. The values of C_f and C_h for each switch position are indicated in the following table:

Switch Position	C_f and C_f'	C_h and C_h'
0	0	360 pF
1	0.001	500
2	0.002	750
3	0.005	0.001 μF
4	0.01	0.0015
5	0.02	0.002
6	0.03	0.0035
7	0.04	0.005
8	0.05	0.007
9	0.10	0.01
10	0.20	0.02
11	0.40	0.03

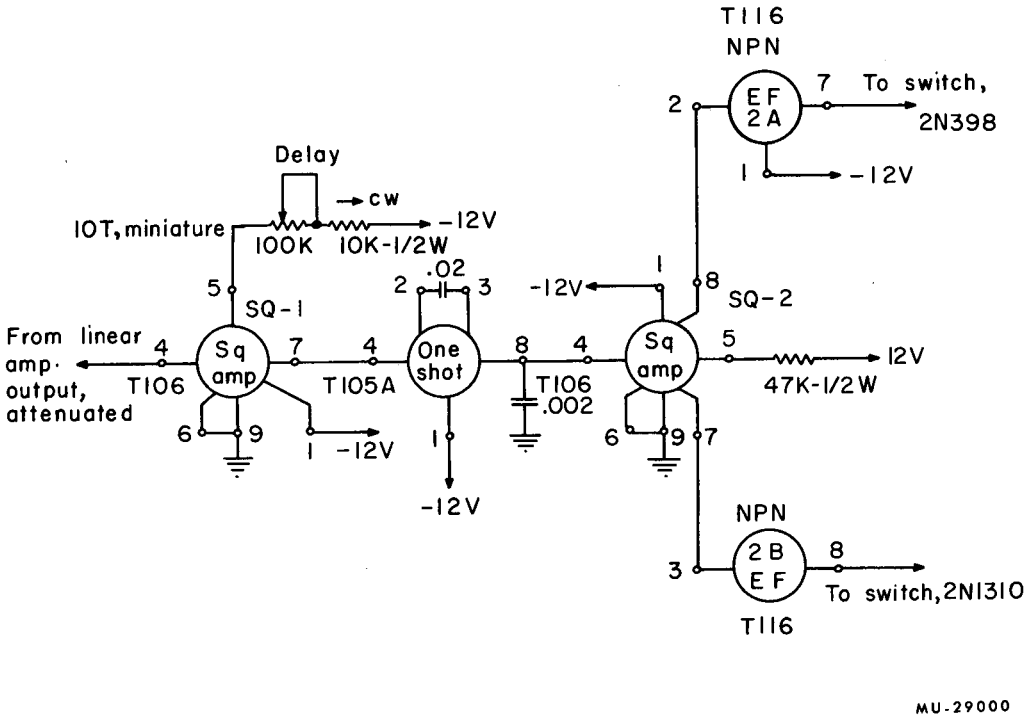

Fig. 35. Gating chain. The circled units are packaged circuits, Engineered Electronics Company, T-series. Pins 6 and 9 connect to ground.

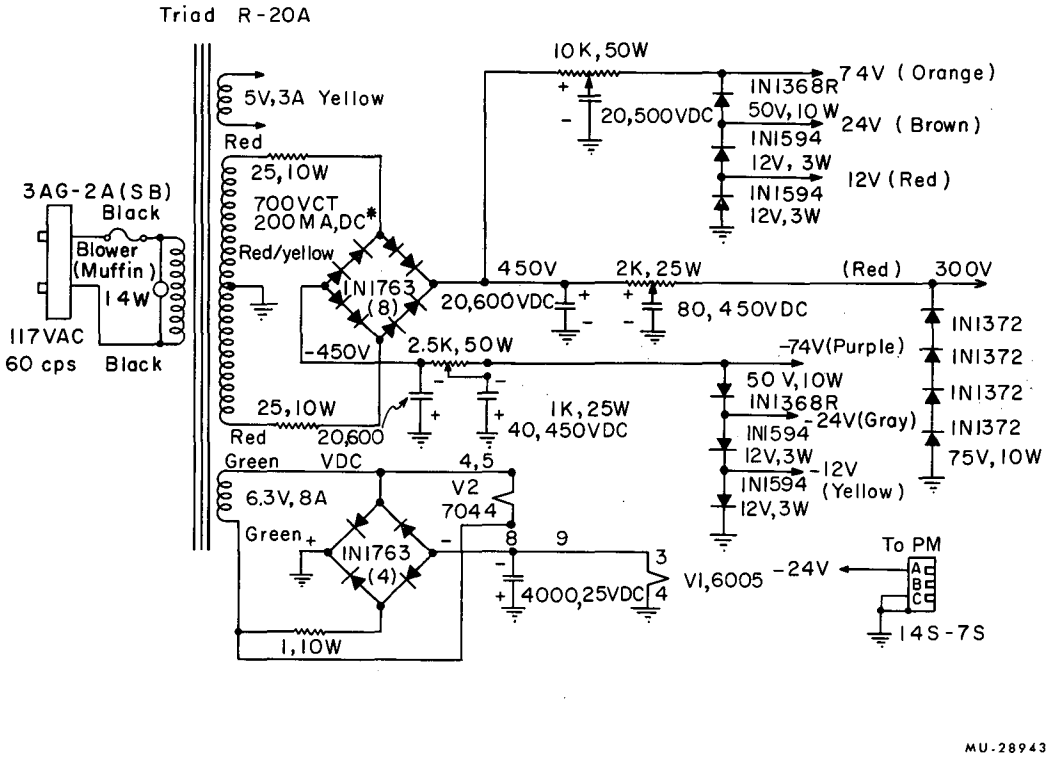

Fig. 36. Power supply. This transformer is slightly overloaded. The eight IN1763's have been replaced by four IN3563's.

REFERENCES AND FOOTNOTES

1. Howard K. Schachman, Ultracentrifugation in Biochemistry (Academic Press, New York, 1959).
2. S. Hanlon, K. Lamers, G. Lauterbach, R. Johnson, and H. K. Schachman, Arch. Biochem. Biophys. 99, 157 (1962).
3. Harold S. Black, Modulation Theory (D. Van Nostrand Company, Inc., New York, 1953), p. 39.
4. Eliahu I. Jury, Sampled Data-Control Systems (John Wiley and Sons, Inc., New York, 1958), p. 48.
5. A rotary head permits selection of one of six slits, each about 0.1 in. long and varying in width from 0.001 to 0.006 inch.
6. Four scanning rates are available. The image is scanned in 6, 10, 18, or 35 seconds.
7. The cells are loaded with regard to rotor rotation.
8. The gating chain had been triggered with pulses from the log amplifier output. Noise impulses were exaggerated and produced spurious triggering.
9. J. Millman and H. Taub, Pulse and Digital Circuits (McGraw-Hill Book Company, Inc., New York, 1956), p. 445.
10. Visicorder is the commercial name for a recording oscillograph. This is a 14-channel unit employing an ultraviolet beam and selfdeveloping paper. Model 906A. Galvanometers are M100-120A with a sensitivity of 10 μamps inch, and a frequency response (flat ±5%) of 0-60 cps.
11. Spinco ultracentrifuge, model E. The speed range is 600 to 67 000 rpm, which corresponds to 260 000 g's at 60 000 rpm.
12. The sample is not always virus, but it will be treated as such here, for purposes of derivation.